NON-CONTACT MEASUREMENT OF SOIL MOISTURE CONTENT USING THERMAL INFRARED SENSOR AND WEATHER VARIABLES

A Thesis Submitted to the

College of Graduate Studies and Research

in Partial Fulfilment of the Requirements

for the Degree of Master of Science in the

Department of Agricultural and Bioresource Engineering

University of Saskatchewan

Saskatoon

Saskatchewan

By

Talal Yasir Alshikaili

PERMISSION TO USE

In presenting this thesis in partial fulfilment of the requirements for a postgraduate degree from the University of Saskatchewan, I agree that the Libraries of this University may make it freely available for inspection. I further agree that the permission for copying of this thesis in any manner, in whole or in part, for scholarly purposes may be granted by the professor or professors who supervised my thesis work or, in their absence, by the Head of the Department or the Dean of the College in which my thesis work was done. It is understood that any copying or publication or use of this thesis or parts thereof for financial gain shall not be allowed without my written permission. It is also understood that due recognition shall be given to me and to the University of Saskatchewan in any scholarly use which may be made of any material in my thesis.

Requests for permission to copy or to make other use of material in this thesis in whole or part should be addressed to:

Head of the Department of Agricultural and Bioresource Engineering,

University of Saskatchewan

Saskatoon, Saskatchewan, S7N 5A9

ABSTRACT

The use of remote sensing technology has made it possible for the non-contact measurement of soil moisture content (SMC). Many remote sensing techniques can be used such as microwave sensors, electromagnetic waves sensors, capacitance, and thermal infrared sensors. Some of those techniques are constrained by their high fabrication cost, operation cost, size, or complexity. In this study, a thermal infrared technique was used to predict soil moisture content with the aid of using weather meteorological variables.

The measured variables in the experiment were soil moisture content (%SMC), soil surface temperature (T_s) measured using thermocouples, air temperature (T_a), relative humidity (RH), solar radiation (SR), and wind speed (WS). The experiment was carried out for a total of 12 soil samples of two soil types (clay/sand) and two compaction levels (compacted/non-compacted). After data analysis, calibration models relating soil moisture content (SMC) to differential temperature (T_d), relative humidity (RH), solar radiation (SR), and wind speed (WS) were generated using stepwise multiple linear regression of the calibration data set. The performance of the models was evaluated using validation data. Four mathematical models of predicting soil moisture content were generated for each soil type and configuration using the calibration data set. Among the four models, the best model for each soil type and configuration was determined by comparing root mean of squared errors of calibration (RMSEC) and root mean of squared errors of validation (RMSEV) values. Furthermore, a calibration model for the thermal infrared sensor was developed to determine the corrected soil surface temperature as measured by the

sensor (T_{ir}) instead of using the thermocouples. The performance of the thermal infrared sensor to predict soil moisture content was then tested for sand compacted and sand non-compacted soils and compared to the predictive performance of the thermocouples. This was achieved by using the measured soil surface temperature by the sensor (T_{ir}), instead of the measured soil surface temperature using the thermocouples to determine the soil-minus-air temperature (T_d). The sensor showed comparable prediction performance, relative to thermocouples.

Overall, the models developed in this study showed high prediction performance when tested with the validation data set. The best models to predict SMC for compacted clay soil, non-compacted clay soil, and compacted sandy soil were three-variable models containing three predictive variables; T_d, RH, and SR. On the other hand, the best model to predict SMC for compacted sandy soil was a two-variable model containing Td, and RH. The results showed that the prediction performance of models for predicting SMC for the sandy soils was superior to those of clay soils.

ACKNOWLEDGEMENTS

TABLE OF CONTENTS

LIST OF FIGURES

ix

LIST OF TABLES

LIST OF NOMENCLATURE

M_c – moisture content [%]

M_d – dry weight of soil [g]

M_t – wet weight of soil [g]

M_w – weight of water [g]

R^2 – coefficient of determination

RH – relative humidity [%]

RMSEC – root mean squared errors of calibration

RMSEV – root mean squared errors of validation

SMC – soil moisture content [%]

SR – solar radiation [$w.m^{-2}$]

T_a – ambient air temperature [°C]

T_d – differential temperature (soil surface-minus-ambient air temperature) [°C]

T_s – soil surface temperature [°C]

T_{ir} – soil surface temperature measured using the thermal infrared sensor [°C]

T_{sens} – sensor body temperature [°C]

Vo – thermal infrared sensor output voltage [mV]

WS– wind speed [m/s]

1. INTRODUCTION

Water is an integral part of all living tissue and is an essential component of fertile soils. Soil moisture is of vital importance for plant growth and also affects the success of seeding, cultivation and harvesting operations (de Jong, 1976). Soil moisture information can be used for reservoir management, early warning of droughts, irrigation scheduling, and forecasting of crop yield. Current contact soil moisture measuring techniques are based on field and point measurements. The extrapolation, transfer, and recording of soil moisture point measurements are inadequate and slow in large fields because soil properties and moisture content vary spatially (Collet, 1976).

The standard method of determining soil moisture is by oven drying the soil at $105^{o}C$. This method is laborious and destructive. De Jong (1976) mentioned four other methods that can be used to measure soil moisture content. The first method is neutron probes, in which high energy (fast) neutrons are emitted into the soil, slowed down, and then the slow neutrons are detected. As hydrogen (H) is a very efficient thermalizer, the slow neutron count provides a measure of the H content, and thus, of the moisture content in the soil. The second method is using porous blocks that are buried in the soil and often used to estimate soil water content or tension. The water in the blocks reaches the same tension as the soil water. This tension can be estimated from properties of the blocks that are related to their moisture content (electrical resistance, weight, permeability to air, etc.). The third method is thermocouple psychrometers (miniature wet-dry bulb thermometers) which can be used to measure the relative humidity of the soil air and from this the

14

total soil moisture tension can be calculated. The last method is electrical resistance, in which the soil moisture content can be inferred from electrical resistance of the soil measured *in situ*: this approach is not very accurate due to changes in salt content of the soil water. Unfortunately, all previously mentioned methods are destructive, laborious, and time consuming. Furthermore, the use of previously mentioned methods requires contact with the soil surface whose moisture content is to be measured, and those methods are incapable of making large area measurements.

Luney and Dill, (1970) reported that remote sensing is the logical non-contact technique for sensing and covering larger areas within a short time period. It has the potential to improve the detection and characterization of many agricultural and forestry phenomena. Recent studies indicate that remote-sensing techniques can be used in many electromagnetic spectrum regions: ultraviolet; visible; infrared; and microwave to collect data that provide a measure of the reflectance, emittance, dielectric constant, surface geometry, and equivalent black-body temperature of plants, soils and water.

According to Holter et al., (1970), remote sensing can be carried out using photographic or non-photographic sensors. Photographic sensors are those sensors that utilize sensitive photographic films (panachromic film, infrared film, false-color film, and color-negative film) to capture various land phenomena. Photographic sensors can be used on the ground, from aircraft, or from orbital satellites. Photographic film is limited in spectral response to the region from the near ultraviolet to the near infrared. On the other hand, non-photographic sensors collect the data in an electrical form and operate in the spectrum region that lies between the

microwave and the ultraviolet spectrum regions. Examples of non-photographic sensors are: passive microwave sensors, active microwave sensors (radars), and infrared sensors. Remote sensing has been used for the measurement of soil moisture content (Davis et al., 1976; Whiting, 1976; Ulaby, 1976; J. Chilar, 1976; Shmugge et al., 1974; Scherer, 1986; Levitt, 1989; Myhre and Shih, 1990).

This research investigated the potential of using a non-photographic thermal infrared sensor to estimate soil moisture content for two types of soils (sand/clay) and two compaction levels (compacted/non-compacted).

2. OBJECTIVES

The goal of this project was to investigate the correlations between the soil moisture content and environmental variables. These environmental variables were soil surface-minus-air temperature (Td), relative humidity (RH), solar radiation (SR), and wind speed (WS) using two types of soil (clay and sand) with two different compaction levels (compacted and non-compacted). Those correlations were then used to develop and test predictive models suitable for implementation with a non-contact infrared temperature sensor in order to predict soil moisture content. The specific objectives of this study were to:

1. develop empirical models to predict soil moisture content of two soil types (sand/clay) and two compaction levels using measurements of environmental variables and

2. investigate the suitability of a non-contact thermal infrared temperature sensor for the purpose of measuring soil temperature and inclusion of these data in an empirical model developed in objective 1, mentioned above.

3. BACKGROUND

3.1 Soil Moisture

Knowledge of the soil water parameters is important for the proper selection of a sensor. Soil moisture content is the amount of water that is held by a soil. The amount of water in the soil determines many of the soil properties. De Jong (1976) reported that the amount of soil moisture – which is utilized by living organisms in the soil - is estimated as only a small fraction of the earth's hydrosphere (table3.1). The moisture in the soil may be present in three phases: liquid, ice, or vapor. However, the most common form of the moisture in soil is liquid.

Table 3.1 Estimated and relative quantities of water in the earth's hydrosphere (Russell and Hurlbert, 1959)

	Hectare-meters	Ratio to annual precipitation
Total water	20500×10^9	1850
Total fresh water	1400×10^9	125
Groundwater to 3800 m	1000×10^9	90
Lakes and streams	15×10^9	1.4
Atmosphere	1.5×10^9	0.14
Soil moisture	0.8×10^9	0.07
Plants and animals	0.1×10^9	0.01
Annual precipitation	11×10^9	1.0
Annual runoff	2.1×10^9	0.2

As the water content of a soil changes, many of the soil properties change accordingly, such as energy level of the soil, and the permeability of the soil. Soil permeability is a measure of the ability of air and water to move through the soil. The soil permeability decreases rapidly with decreasing moisture content since the flow of water is restricted to smaller pores and thinner films (De Jong, 1976). The temperature of the soil moisture also has an effect on some of the soil's properties. At a given soil moisture, a decrease in soil temperature causes an increase in soil water tension. Data by Taylor (1966) and Taylor et al., (1961) indicated that at 20°C, soil water tension increases 1 to 5 % with every 1°C decrease in temperature, and the effect increases with decreasing moisture content. The permeability of soil to water decreases with decreasing temperature as is to be expected from the effect of temperature on viscosity. Carry and Taylor (1967) reported that the viscosity of soil water is more temperature dependent than free water viscosity and this dependence increases at low soil moisture contents. Soil moisture is expressed on a weight basis (g/100g oven dry soil) or on a volume basis (cm^3/100cm^3 bulk soil).

3.1.1   Typical soil moisture measuring techniques

A variety of methods and techniques is available for measuring soil moisture content. The selection of the method and equipment will depend on ease of use, cost of equipment, and a desire to monitor continuous changes in soil moisture. Examples of typical soil moisture content measuring techniques are:

1. *Gravimetric method:* The gravimetric method is a direct technique for estimating the total moisture content of soils. This method involves drying a soil sample in an oven (105°C for 24 hours) to determine the soil moisture content. Water content (grams of water in the sample) equals the initial field

soil weight minus the oven-dry weight. Water content (%) can then be calculated by dividing the sample water content (grams) by the initial field soil weight (grams) and multiplying by 100.

Advantages: This technique is relatively inexpensive, simple, and highly accurate.

Disadvantages: This technique is time-consuming, destructive to the soil, labor-intensive, and difficult in rocky soils. A lab oven or microwave oven, soil sampling equipment, and lab scale are required.

2. *Neutron Probe:* A radioactive source (Americium 241) is inserted into the soil, from which fast neutrons are emitted towards the soil. When those fast neutrons collide with the hydrogen atoms present in the water molecules, fast neutrons lose their energy and become slow. Those neutrons have no charge and cannot directly be detected. Therefore, a gas (boron tri-fluoride) is used to absorb those slow neutrons which make the gas nucleus emit photons that are proportional to the number of absorbed neutrons. The resulting photons are detected using an electronic device. The electronic counting device is used to measure the number of photons, which is proportional to the number of slow neutrons, which is proportional to the amount of moisture present in the soil.

Advantages: The neutron probe allows a rapid, accurate, repeatable measurement of soil moisture content to be made at several depths and locations.

Disadvantages: The major disadvantages are the use of radioactive material requires a licensed and extensively trained operator, the contact with the soil

surface, the very high equipment cost and the extensive calibration required for each site.

3. *Gypsum-porous blocks:* Soil moisture blocks operate on the principle that the electrical resistance of a porous block is proportional to its water content. Ceramic thermal dissipation measures the rate of heat dissipation in the soil, which correlates to soil moisture content.

   Advantages: The method is quick, repeatable, and relatively inexpensive.

   Disadvantages: The blocks do not work well in coarse-textured, high shrink-swell or saline soils and are destructive to the soil. Accuracy of gypsum-porous blocks is poor. The blocks should be replaced every 1 to 3 years. The sensitivity of the blocks is poor in dry soil conditions. The blocks need to be soaked in water for several hours before installing them in the field.

4. *Tensiometers:* A tensiometer is an airtight hollow tube filled with water. A porous ceramic cup is attached to the end of the tube which is then inserted into the soil, and then a vacuum gauge is attached to the upper end. The tensiometer measures soil moisture tension, and provides an index of how tightly water is held in the soil. A soil moisture retension curve is developed for each horizon of the soil to determine soil water content.

   Advantages: Tensiometers are not affected by the amount of salts dissolved in the soil water. Tensiometers measure soil moisture tension with reasonable accuracy in the wet range.

   Disadvantages: Tensiometers only operate between saturation and about -70kPa level of soil moisture content which makes them not suitable for measurements in dry soils. In addition, tensiometers are destructive to the soil surface.

5. *Time-Domain Reflectometry (TDR):* The TDR is a portable device which can be used to make point soil moisture measurements or can be linked to a multiplexer to measure the soil moisture content of an array of buried waveguides (Heimovaara and Bouten., 1990). TDR probes (waveguides) are used as sensors that are buried into the soil whose moisture content is to be measured. An electromagnetic wave is sent through these probes. Reflection of the applied signal will occur where there are impedance changes. The impedance value is related to the geometrical configuration of the probe and inversely related to the dielectric constant of the soil. A change in volumetric water content of soil surrounding the probe causes a change in the dielectric constant. The change of the dielectric constant of the soil, changes the probe impedance which affects the shape of the reflected signal. The shape of the reflected signal contains information that is used to determine soil moisture content.

Advantages: TDR is accurate, provided continuous measurements, no calibration is needed, and is unaffected by salts.

Disadvantages: TDR is destructive to the soil being tested, contains complex electronics, and expensive equipment is required for good measurements.

3.2 Remote sensing

Remote sensing is a term that is used for the study of remote objects from a distance. It denotes the employment of modern sensors and data processing. The use of remote sensing has replaced some contact and destructive methods in sensing environmental and agricultural phenomena. There are many remote sensing techniques that can be used in the infrared and microwave spectral regions in order to collect data from

targeted locations. Luney and Dill (1970) reported that remote sensing can be used for the detection and characterization of agricultural and land phenomena. Remote sensing of surface soil moisture still is not widely used, although the theory and techniques to develop this important remote sensing resource are well established in soil and water sciences literature (Ulaby et al., 1982; deGriend and Owe, 1994).

3.2.1   General applications of remote sensing

Luney and Dill, (1970) discussed the main uses of remote sensing in agricultural and water management sectors as follows:

- *Land-Use Inventories:* In many countries, air photos are used to make maps that show the distribution of plants, specific crops, and land use.

- *Soil Surveys:* Before 1930, soil surveys in the United States took a long time due to the use of traditional field-methods for soil classification and land mapping. With the use of air photos, soil information could be acquired more quickly and efficiently (U.S Soil Conservation Service, 1966).

- *Crop Condition Estimates and Yield Forecasting:* Remote sensing facilitates the process of obtaining data on crop yields as well as forecasts during the growing season. These data are very important to agriculture because they affect all phases of agricultural production, processing, and storage.

- *Water-Supply Information and Management:* Remote sensing is used for the management of water resources. It is used to find fresh water at low sensing cost, to forecast the future supply, and to control the location, quantity, quality, and timing of that supply.

- *Irrigation Management:* Remote sensing techniques can be used to monitor the changes of moisture levels in the soil and to detect the water-table depths with enough confidence (Myers, 1967). This information is then used to

23

advise the farmers on irrigation timing and the amount of moisture present in the soil, so that they can avoid over-application or under-application of irrigation water.

3.2.2   Remote sensing of soil moisture

Gates (1970) reported that there are two properties of a soil surface which are of general interest in remote sensing. The first property is the soil reflectance of incident radiation and the second property is concerned with its long-wave emittance and surface temperature. According to Gates (1970), "the reflectance of a soil depends upon its coloration, texture, roughness, moisture content, mineral and chemical composition, angle of illumination, and degree of shadowing by plants or buildings"(Gates 225-252).

Because soil moisture is one parameter that affects the reflectance and emittance of soil, then this effect implies that a change of water content in a soil causes a change in its reflectance and/or emittance. An appropriate remote sensing technique can be used to detect and measure the change in reflectance and/or emittance of the soil and relate it to the amount of moisture present in the soil. A calibration model can be developed to predict soil moisture content which relates soil moisture content to soil reflectance (Ulaby, 1975; Schmugge et al., 1974) or to differential temperature (Td) and weather meteorological variables (Shih et al., 1986; Myhre and Shih, 1990).

3.2.3 Types of remote sensing

Remote sensing can be carried out using sensors that are categorized into two main categories: photographic and non-photographic sensors (Holter et al., 1970).

3.2.3.1 Photographic sensors

Photographic sensors are those sensors that utilize sensitive photographic films such as panachromic film, infrared film, false-color film, and color-negative film to detect various land phenomena, whether it is used on the ground, from aircraft, or from satellites. According to Holter et al., (1970), photographic sensors have two serious limitations in remote sensing applications. First, the output is a photograph, which makes the process of interpretation and discrimination analysis difficult. Second, photographic film is limited in spectral response to the region from the near ultraviolet to the near infrared. Therefore, photographic sensors are not suitable for night-time operation unless artificial light sources are used for illumination. Moreover, clouds, fog, and smoke are obstacles in this spectral region, so sensing the ground from a very high altitude is sometimes difficult and often impossible.

3.2.3.2 Non-photographic sensors

Non-photographic sensors are those sensors that operate in portions of the electromagnetic spectrum from the microwave to the ultraviolet region. Infrared, passive-microwave, and radar sensors operate under both day and night conditions, and their sensing ability is not seriously affected by clouds and bad weather. Because the data are collected in electrical form, they are easily transmitted to a remote location. In addition, signals for discrimination analysis can be processed easily with electronic circuits.

3.3 Microwave sensors

Microwave sensors are based on the interaction of the electromagnetic fields with the dielectric and power dissipative properties of a matter, particularly of water. The intensity of the emitted radiation is proportional to the product of the multiplication of temperature and the emissivity of the surface. There are two types of microwave sensors: passive microwave sensors and active microwave sensors (Radars). Passive microwave sensors utilize the natural radiation from the targeted objects or locations and operate in the spectral region between 0.1mm–3cm. On the other hand, active microwave sensors (Radars) provide their own source of radiation by sending an electromagnetic wave to the target and measure the reflected radiation. Holter et al., (1970) reported that radars have the greatest advantage because they can be used to conduct remote sensing of soil surface in bad weather, anytime in the day, and without concern for problems of interpretation associated with differences between day and night thermal patterns of the soil surface. The electromagnetic waves of microwave sensors can penetrate clouds, smoke, fog, and precipitation because they have long wavelength (higher than 0.5 cm).

3.3.1 Use of microwave sensors for soil moisture content measurement

There were many research studies carried out to evaluate the possibility of using passive and active microwave sensors for the detection of soil moisture content in soils such as ground-based (Jackson and O'Neill., 1990; Wigneron et al., 1995), aircraft-based (Jackson et al., 1999; ONeill et al., 1996) and space-based sensors (deGriend and Owe, 1994; Njoku et al., 2000). Those experiments were carried out with microwave sensors operating at low frequencies (<6 GHZ). Furthermore, many efforts have been made to correlate soil moisture with several parameters that can be

remotely sensed by microwave sensors, such as surface albedo (Idso et al., 1975), the diurnal range of surface temperature (Idso et al., 1975), microwave backscatter coefficient (Ulaby et al., 1974), and microwave emissivity (Schmugge et al., 1974).

3.3.2 Microwave backscatter coefficient as an indicator of soil moisture content

An experiment was done using a 4-8 GHZ truck-mounted active microwave spectrometer to estimate soil moisture content. Preliminary measurements were conducted in 1972 to evaluate the radar response to soil moisture content. Data were acquired over the 0° (nadir) to 70° angular range for both bare fields (Ulaby et al., 1974) and vegetated fields (Ulaby, 1975) as a function of time. The results of the experiment indicated good correlation with moisture content, particularly at small angles of incidence, and the covering band 2.5-8 GHZ was used to acquire detailed data over the 0° - 40° angular range from each of three fields with distinctively different surface roughness. A total of about 40 data sets were acquired, covering a wide range of moisture contents (Ulaby and Batlivala, 1976). To further verify the validity of these results, the system frequency was expanded to cover approximately 3 octaves, 1 GHZ to 8 GHz. Five different surface roughness levels were used instead of three, and a total of 85 data sets were acquired from vegetation crops (wheat, milo, corn and soybeans) over their growing cycle.

For bare soil, the results showed that the scattering coefficient increased with the soil moisture content at all angles, frequencies, and polarizations if the soil surface roughness remained unchanged (Ulaby, 1975; Ulaby and Batlivala, 1976). On the other hand, variations in scattering coefficient due to the change in surface roughness

were considerable, when using five different roughness levels of soil surface having the same level of moisture content (Batlivala and Ulaby, 1976). Ulaby (1976) concluded that the optimum sensor parameters for mapping soil moisture for bare soils were: frequency range of 3.5-4.5 GHZ , angle of incidence range of 7°- 17° , and polarization = HH).

Ulaby (1976) described the backscattered power received by radar viewing a bare soil surface of an area A in the direction θ (relative to nadir) by the following equation:

$$P_r = \left(\frac{P_t G_t G_r \lambda^2 A}{(4\pi)^3 R^4} \right) \sigma^\circ \tag{3.1}$$

where:

P_r = transmitted power in watt [W],

P_t = transmitted power in watt [W],

G_t and G_r = transmit and receive antenna gain, respectively,

λ = signal wavelength in meter [m],

R = range to the cell A in meter [m], and

σ° = scattering coefficient in decibel [dB].

The scattering coefficient is the only parameter which relates the terrain back scatter to the received power by a microwave sensor. The scattering coefficient is determined by soil surface characteristics such as the roughness of the soil and the soil power reflection coefficient. However, the soil power reflection coefficient is a function of the dielectric constant of soil, and the dielectric constant of the soil is dependent on the soil moisture content.

28

For vegetation-covered soil, Ulaby (1976) mentioned a model (equation 3.2) that can be used to evaluate the requirements for mapping the moisture content of the soil underlying a vegetation cover. The total scattering coefficient for a soil with a vegetation cover, as measured by radar, is assumed to consist of two components as follows:

$$\sigma°(\theta) = \sigma_v°(\theta) + \sigma_s°(\theta)e^{-4\alpha h \sec \theta} \tag{3.2}$$

where:

$\sigma_v°(\theta) =$ vegetation scattering coefficient at angle θ,

$\sigma_s°(\theta) =$ soil scattering coefficient at angle θ in the absence of vegetation cover,

$\alpha =$ field attenuation coefficient of the vegetation, and

$h =$ canopy height.

Ulaby (1976) found that the penetration of the microwave sensor signal through a vegetation canopy decreased with frequency and angle of incidence. He indicated that to minimize field attenuation (α), lowest frequencies and angles of incidence should be used.

3.3.2.1   Factors affecting Microwave sensors backscatter

The main factor which affects backscatter to a microwave sensor is soil moisture content. Ulaby (1975) and Ulaby and Batlivala (1976) reported that if the soil surface roughness remains unchanged, the scattering coefficient $\sigma°$ generally increases with moisture content at all incidence angles. There are other two factors that can affect the radar backscatter from a terrain surface: terrain geometry and electrical (dielectric) properties. However, for a vegetative covered surface, the backscatter is also affected by vegetation and the underlying soil.

3.4 Thermal Infrared sensors

Infrared radiation is an electromagnetic radiation of a wavelength longer than that of visible light and shorter than that of radio waves. Infrared radiation has wavelengths between approximately 750 nm and 1 mm (Liew, 2006). The infrared portion of the spectrum has a number of technological uses, including target acquisition and tracking by the military, remote temperature sensing, wireless communication, spectroscopy, and weather forecasting. Thermal infrared sensors measure the infrared radiation emitted by the object and the energy is directly related to the object's temperature.

3.4.1 Use of Infrared thermometry to estimate soil moisture content

The use of thermal infrared sensors to estimate soil moisture content has only recently been studied. Soil moisture content and soil surface-minus-air temperatures can be correlated together through thermal properties of the soil (Myhre and Shih, 1990).

The infrared thermometry technique involves the measurement of soil surface temperature and air temperature using a thermal infrared sensor. Then, the soil surface-minus-air temperature (Td) is calculated. The calculated soil surface-minus-air temperature is related to the amount of soil water present where soil surface and air temperatures are taken. Other meteorological variables like solar radiation, relative humidity, and wind speed, are also measured simultaneously. Measurements of those variables are taken at different levels of moisture content, soil surface and air temperatures, and other weather related meteorological variables. A calibration model is then developed which relates soil moisture content as the dependent

variable to T_d, and the rest of weather variables can be incorporated into the calibration model to enhance prediction performance.

Shih et al. (1986) used multiple linear regression to evaluate the importance of using air and grass/soil temperature, solar radiation, wind speed, and relative humidity in estimating soil water content. Shih et al. (1986) concluded that temperature and solar radiation were important parameters needed to estimate soil water content, while wind speed and relative humidity were not important in Florida, where the experiments were performed. They also reported that using a plant surface-minus-air temperature would be more accurate than using either the plant surface temperature or air temperature alone.

3.4.2   Surface–minus-air temperature as an indicator of water content

The relation between the differential temperature (surface-minus-air) and soil/plant parameters was first closely studied in the mid-1970s. Idso and Ehler (1976) concluded that soil moisture content could be predicted for sorghum during the soil drying cycle using plant surface–minus-air temperature measurements.

Soil water content and surface-minus-air temperatures can be related through the thermal properties of the soil and water. Gillespie and Kahhle (1977) indicated that because water has a higher specific heat and resulting in a higher thermal capacity than soil, a wetter soil will have higher thermal capacity and conductivity. Thermal inertia, which is a function of heat capacity and thermal conductivity, is a measure of the ability of a substance to absorb and transfer heat energy. Therefore, as soil water content increases, the thermal inertia also increases. A soil with a high thermal inertia

(due to a higher soil water content) will be able to transfer a greater radiant heat load from the soil surface to the soil subsurface than a soil with a low thermal inertia. As the heat energy is transferred away from the soil surface, the surface temperature will decrease. Thus, soil water content is correlated to air and daytime surface temperature (Shih et al., 1986). Also, as wind speed increases, the ability of the soil surface to dissipate heat energy increases.

The best time to make measurements of Td is when the difference between soil surface temperature (Ts) and air temperature (Ta) is the greatest. Many studies have been done to monitor the temperature fluctuations during the day. Temperature graphs show that soil/plant surface temperatures are greater during the middle of the day. On the other hand, air temperature is generally greater than soil/plant surface temperature in the morning and afternoon. Myhre (1988) found that the optimal time to measure surface-minus-air temperature in Florida was between 11:00 A.M and 2:00 P.M. Other studies recommended that the optimal times for measurement of plant surface-minus-air temperatures were at 2:00 P.M (Ehrler et al., 1978) and between 1:00-3:00 P.M. (Blad et al., 1978).

Myhre and Shih (1990) used multiple regression analysis to develop a calibration model that related soil moisture content to the independent variables: differential temperature (Td); solar radiation (SR); relative humidity (RH); and wind speed (WS). They discussed and analytically explained the energy balance equations that were developed by Mahrer and Pielke (1977) and McCumber and Pielke (1981). Those equations provided the basis for the calibration models developed by Mahrer and Pielke (1977) and McCumber and Pielke (1981) to estimate soil moisture

content. The energy balance at the soil surface as developed by McCumber and Pielke (1981) is given as follows:

$$R_s + R_1 - \sigma(Tg^4) + \rho LU_* Q_* + \rho C_p U_* TH_* - \rho_s C_s K_s (\partial T / \partial Z)_G = 0 \qquad (3.3)$$

where:

R_s = incoming solar radiation [W.m^{-2}],

R_1 = incoming longwave radiation [W.m^{-2}],

σ = Stefan-Boltzman constant = 5.670×10^{-8} [W.m^{-2}.K^{-4}],

Tg^4 = soil surface temperature [K°],

$\rho LU_* Q_*$ = turbulent latent heat flux [W.m^{-2}],

$\rho C_p U_* TH_*$ = sensible heat flux [W.m^{-2}], and

$\rho_s C_s K_s (\partial T / \partial Z)_G$ = soil heat flux [W.m^{-2}].

Myhre and Shih (1990) reported that equation (3.3) represents the terms used in the soil water content estimation models. The first two terms (R_s and R_1) involve solar radiation as a variable. The third term is the emitted long-wave radiation ($\sigma(Tg^4)$), which is a function of the ground surface temperature. The turbulent latent heat flux term ($\rho LU_* Q_*$) is dependent upon wind speed and relative humidity of the air above the surface, while the sensible heat flux ($\rho C_p U_* TH_*$) is dependent upon air temperature and relative humidity. The soil heat flux ($\rho_s C_s K_s (\partial T / \partial Z)_G$) is dependent upon the physical soil properties and water content. The flow of heat through the soil is dependent upon the thermal inertia of the soil which is a function of the thermal conductivity and the volumetric heat capacity (Vleck and King, 1983). The effect of soil moisture content on thermal conductivity and thermal inertia are

related as follows: as soil moisture content increases, thermal conductivity and thermal inertia also increases.

Based on the previous discussion, Myhre and Shih (1990) reported that equation 3.3 can be written as:

$$WSWC = f(TD, SR, WS, RH) \quad .\tag{3.4}$$

Equation 3.4 relates the weighted soil water contents (WSWC), as a function of depth, to temperature difference (Td), solar radiation (SR), wind speed (WS), and relative humidity (RH).

Myhre and Shih (1990) indicated that if experimental data of temperature difference (Td), solar radiation (SR), wind speed (WS), and relative humidity (RH) are available, the coefficients of each variable in the equation can be estimated using multiple linear regression analysis. The multiple linear regression model is used because it is simple compared to other models like the polynomial and non-linear regression models. Moreover, linear models calculate the unknown parameter (dependent variable) faster when it is incorporated into the sensor system, which is an important factor for fast remote sensing of soil moisture content during operation in the field. The developed and used models by Myhre and Shih (1990) to estimate soil moisture content took the following form:

$$WSWC = a_0 + a_1 TD + a_2 SR + a_3 WS + a_4 RH \quad .\tag{3.5}$$

3.4.3 Use of thermal infrared sensor and weather meteorological variables to estimate soil moisture content

For their experiment, Myhre and Shih (1990) used 24 lysimeters (non-weighed) located at the University of Florida irrigation park. Those lysimeters contained Arredondo fine sand (loamy, siliceous, hyperhermic, Grossarenic paleudults). The lysimeters were 1.80m deep and 1.63 m in diameter. Furthermore, aluminum access tubes were inserted in each lysimeter. These access tubes were used for neutron probe measurements. The treatments of the experiment were irrigation amount, presence or absence of clipped Pensacola Bahiagrass (*Paspalum notalum*) and/or a 2 year-old Valencia orange tree (*Sinensis osbeck*). The orange tree shaded only 5% of the lysimeter surface area.

For soil surface temperature measurements (T_s), the soil/plant surface measurements were taken at a height of 1.5 m and at an angle of 45 degrees above the surface of the lysimeter using a hand-held infrared sensor. The temperatures were measured between 11:00 am and 2:00 pm when the sky was clear (no clouds). Measurements were done at temperature ranges of 29^oC-33^oC, solar radiation ranges of 525-$930w/m^2$, and relative humidity of 40-80%. Measurements were carried out for 20 days from June to September, with a total of 20 observations per site. Multiple regression analysis was used for data analysis. Finally, an empirical model was generated for each site that correlated moisture content with the weather meteorological variables.

The results showed average determination coefficients (R^2) of 0.62, 0.61, 0.63 and 0.60 for moisture measurement depths of 0.15, 0.30, 0.60, and 0.90 m, respectively.

Myhre and Shih (1990) concluded that the use of solar radiation, wind speed, and relative humidity in addition to soil/plant surface-minus-air temperature difference did not significantly increase the accuracy of the soil water content estimation. Also, Myhre and Shih (1990) concluded that for moisture measurement depths of 0.60 m, and 0.90 m, the use of ratio of plant/soil surface-minus-air temperature measurements divided by solar radiation improved the soil moisture content estimate.

3.5   Summary

From the above study, it appears that thermometry is a useful non-contact tool for remote sensing of soil moisture content. Thermal infrared sensors used for infrared thermometry are more advantageous than microwave sensors in that they are smaller, less complex in terms of electronics and lower in cost. This technique, when used for estimating soil moisture content, has not been widely accepted, although previous work done by Shih et al. (1986), Scherer (1986), and Myhre and Shih (1990) showed positive and promising results.

3.6   Quantitative analysis of data

Because of the large amount of available data from the measured variables in this project, there is a need for quantitative data analysis to develop calibration models that reflect the correlation between the dependent variable and the independent variables and also to predict the value of the dependent variable for given values of the independent variables. The goal behind the data analysis in this project is to create and test calibration equations of the measured data using a thermal infrared technique for the given samples of soils of different types (clay and sand) and different compaction levels (compacted and non-compacted). The challenge is then

to identify the calibration model that most accurately reflects the relationship between soil moisture content and the measured variables. These equations can be used later to accurately predict the soil moisture content of a given soil surface measured in the same manner (technique).

There are many effective calibration models including linear, polynomial, and non-linear models. Among the possible models, linear ones are the most familiar and simplest to employ, while providing comparable predictive performance.

3.6.1 Calibration and validation

Calibration is the process of generating a model that best relates the measured dependent variable (soil moisture content) to the measured independent variables (differential temperature (Td); relative humidity (RH); solar radiation (SR); and wind speed (WS). On the other hand, validation is the process of testing the performance of the generated model to predict soil moisture content using a new set of data called the validation data set.

The process of generating a predictive model involves the partition of the data into two portions. The first part is the calibration set. The calibration set is used as a training set from which to generate the calibration models. The remaining portion is the validation set, which is used for testing the performance of the developed model. Duckworth (1998) reported that using a validation set that is not used in the calibration process for testing the generated models gave the best estimate of the model's performance. This is because none of the samples in the validation set were used to develop the model.

Ingleby (1999) reported that when dividing the available data into the calibration and validation sets, it is important to ensure that they both represent the full range of possible values of the dependent variable so that the validation testing will be valid for the whole range of data predictions. This can be achieved by randomizing the raw data prior to dividing them into the calibration and validation sets.

3.6.2   Multiple linear regression analysis

Multiple linear regression (MLR) is a modeling method that relates the variation in each response (the dependent variable, Y) to the variation of one or several variables (the independent variables, X) (Dagnew, 2002). MLR analysis is used to produce a linear calibration model by fitting a linear equation to the calibration data set such that it minimizes the root mean of sum squared errors between the predicted and the actual values of the dependent variable.

The generated models after the linear regression process (calibration process) take the following form:

$$y = a_0 + a_1 x_1 + a_2 x_2 ..., \tag{3.6}$$

where:

y = the dependent variable,

a_0, a_1, a_2 = regression coefficients, and

x_1, x_2 = the independent variables.

3.6.3 Evaluating the model performance

There are many quantitative factors that can be used to evaluate the model's performance: coefficient of determination (R^2) of the model, root mean of squared errors of calibration (RMSEC), and root mean of squared errors of validation (RMSEV). R^2 represents the degree of fitness of the measured data to the regression line. It explains how much of the variability in the dependent variable can be explained when related to the independent variables using that regression line (linear equation). RMSEC and RMSEV are the root mean of squared errors of the differences between the predicted values and the measured ones in the calibration and validation sets, respectively.

The evaluation of a model performance requires comparing the calibration (R^2, RMSE) values and the validation (RMSEV) value. A minimum difference between the two values is indicative of high predictive performance and vice versa.

.

3.6.4 Regression (REG) procedure using SAS®

The SAS® software is a standard statistical program that may be used to analyze data. The multiple linear regression process in this program is used for data analysis (calibration) and to select the appropriate number of variables that gives the best predictive model. It selects the model with the largest R^2 for each number and combination of variables considered (SAS, 1999).

4. MATERIALS AND METHODS

4.1 Experiment field location

The experiment was carried out at the University of Saskatchewan in the parking lot near the Department of Agricultural and Bioresource Engineering. A small outdoor area was reserved to install the experimental setup. This area has a geographical location of 52^0 07' 58.22" N 106^0 37' 38.96" W. The experimental setup included the weather station for the measurement of weather variables, soil carrying and weighing instruments, non-contact thermal infrared sensor, and the data logger. Many considerations have been set to select the experimental location. It was important to choose a location near the University so as to be close to the necessary facilities like power, water, and laboratories. The experiment location was far enough away to ensure that the buildings would not be an obstacle against wind and solar radiation during the day.

4.2 Weather monitoring station

The weather monitoring system (ZENO$^®$-3200) was used to measure and record environmental variables which were, air temperature (T_a), relative humidity (RH), wind speed (WS), and solar radiation (SR). This weather station is small, rugged, practical, and easy to move from one place to another. It consists of sensors, a built-in data logger, battery, and a solar cell for charging the battery. The laptop and the weather station's data logger were connected together using a serial communication protocol and an Rs-232 cable.

The process of programming and the transfer of data to and from the weather station were acquired by using communication software called Hyper Terminal which is provided with Windows operating system (Microsoft Corporation, 2002). The weather station's data logger was programmed to read and measure the environmental variables at a rate of 1 sample/10 seconds. The weather station and all of its accessories are shown in figure 4.1.
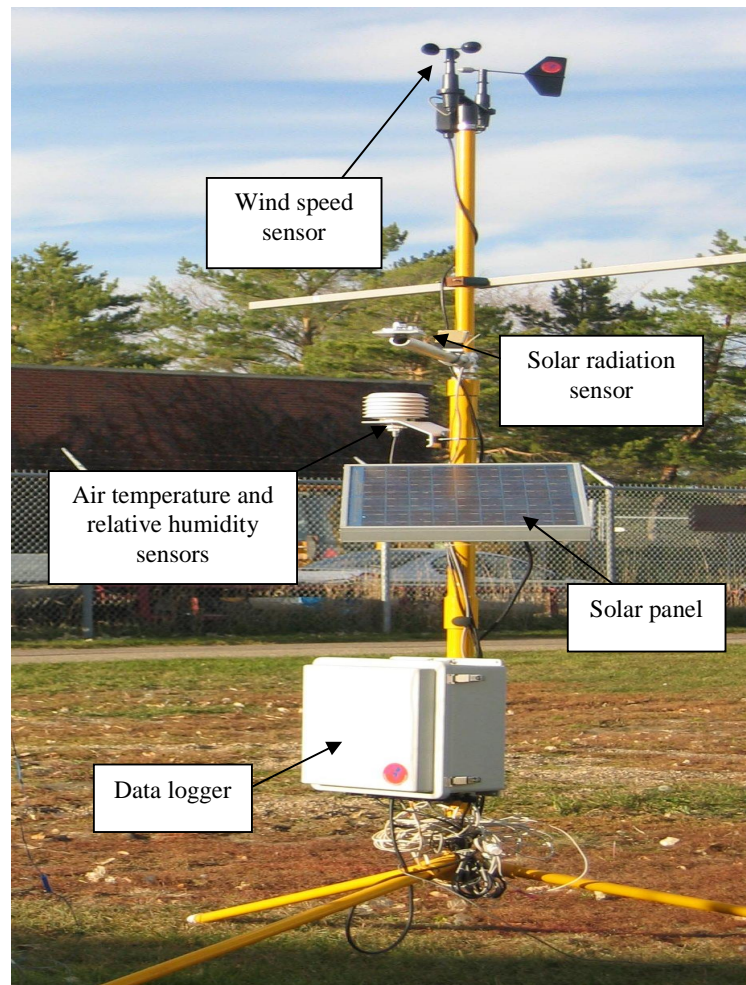
Figure 4.1 ZENO®-3200 agricultural weather monitoring system

4.3 Load cell

A load cell is a sensor which uses strain gauges that are mounted in a specific pattern to provide a meaningful value of the change in pressure or weight. A bending beam load cell (Interface™, Model MB-50), as shown in figure 4.2, was used to measure the change of soil weight during the experiment. The load cell was bolted to a support through two mounting holes at one end. The load (soil container) was applied to the opposite end from the mounting holes. A loading button was inserted in the loading hole by which the load was carried.

Figure 4.2 The (Interface™, MB-50) mini-beam bending load cell

4.3.1 Calibration of the load cell

The load cell was calibrated using known weights of 2406 g and 455 g. For the calibration, the load cell was connected to the data logger through a differential input channel and was supplied with 5 volts of excitation voltage. The known weights were then hung on the loading button of the load cell, one after the other, and the output voltage was then recorded. Using Microsoft® Excel 2003 spread sheet, linear regression analysis was then used to develop a calibration model that correlated the weight and the output voltage. Equation 4.1 is the generated calibration equation. It

was installed in the data logger software and was used for accurately monitoring and measuring the weight change of soil during the experiment.

$$W_t = 740V_o - 163 \qquad\qquad\qquad \textbf{(4.1)}$$

where:

W_t = weight [g], and

V_o = load cell output voltage [mV].

4.4   Support and carrying plate

A 4-link support was fabricated to provide a means of support for the carrying plate. The load cell was attached to the support as shown in figure 4.3 through its mounting holes. A carrying plate fabricated from metal had a rectangular shape and carried the soil container during the experiment. It was hung on the load cell using plastic ropes that were attached to its four corners. A complete schematic diagram showing this setup is given in figure 4.4. For the purpose of fixing and holding the infrared sensor during the experiment, a holder was fabricated with the ability of modifying its height as required.
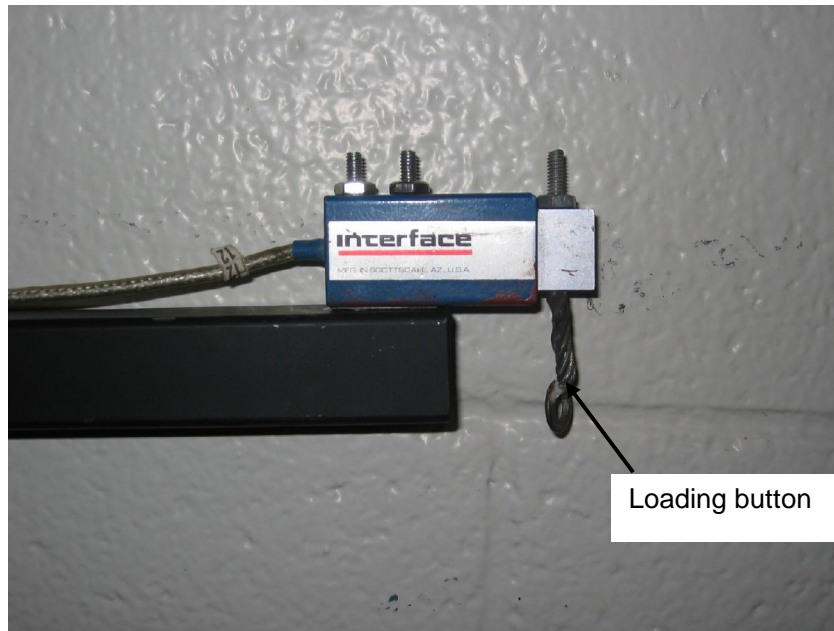
Figure 4.3 Load cell installed on the support
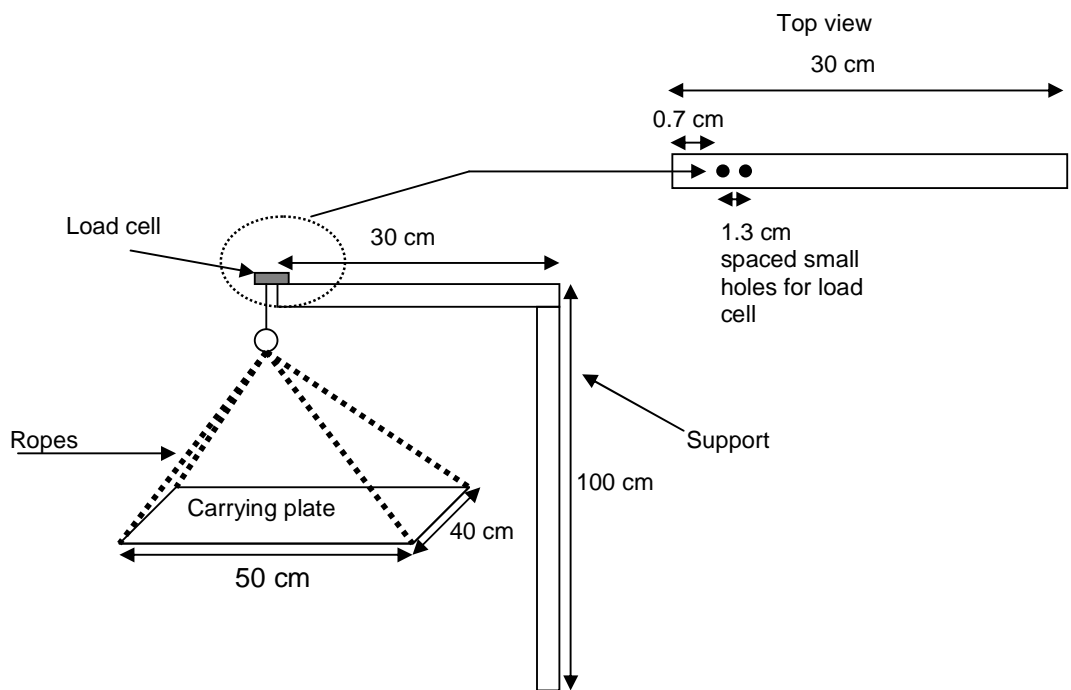
Figure 4.4 Schematic diagram shows the dimensions of the support and the carrying plate

4.5 Soil preparation

The two soil types that were used were: clay and sand, with two different compaction levels: compacted and non-compacted. Before the experiment, the soil was dried at $105^{\circ}C$ for 24 hours using an oven. After drying, the dry weight was determined and then it was left to cool. This step ensured that there is no stored heat from the oven which might affect surface temperature, and also to create an equilibrium situation with the surrounding environment. At early morning, the soil was weighed to measure the amount of water condensed from the surrounding atmosphere that could increase the soil moisture content after being dried.

4.6 Soil compaction

Two soil configurations were used for each soil type: compacted and non-compacted. The compaction was applied before the application of water and the soil was compacted while it was in the container. A square metallic plate, having the same surface area ($1033\ cm^2$) and shape of the container, was put on top of soil surface and pressure was applied on the soil using a load of 44.8 kg, giving a pressure of 4.34 kPa.

4.7 Moisture application and adjustment

For the experiment, the required initial soil moisture content (SMC) was 20% (wet basis). Water was added to the soil by pouring it evenly on its surface and this process guarantees that water is evenly spread on the surface. The mass of water (M_w) that should be added to make 20% soil moisture content can be calculated from deriving the following equation:

$$M_c = \frac{M_t - M_d}{M_t} \times 100 \qquad\qquad (4.3)$$

Because the initial moisture content required was 20%, then

$$0.2 = \frac{M_t - M_d}{M_t} \qquad\qquad (4.4)$$

$$M_t - 0.2M_t = M_d \qquad\qquad (4.5)$$

$$M_t = \frac{M_d}{0.8} \qquad\qquad (4.6)$$

Then the amount of water to be added can be calculated as follows

$$M_w = M_t - M_d \qquad\qquad (4.7)$$

where:

M_t = Total mass of the soil (soil dry mass + water mass) [g],

M_d = Dry mass of the soil [g],

M_c = moisture content [%], and

M_w = amount of water [g].

The condensed water present during the cooling process was subtracted from the calculated water amount.

4.8 Non-contact thermal Infrared sensor for the remote sensing of soil surface temperature

For a remote soil surface temperature measurement, a thermal infrared sensor (Omega, Model OS43, Saskatoon, Saskatchewan) was used. This device is designed for applications where contact measurements are not feasible or non-contact measurement of surface temperature is required. Many considerations had been taken

for the selection of the thermal infrared sensor. Since this sensor was to be used in outdoor conditions, the main consideration was the immunity of the sensor against harsh environmental variables such as temperature, humidity, rain, and solar radiation. Other considerations were accuracy, repeatability, spectral response, response time, and temperature range that can be measured by the sensor. The selected sensor is capable of measuring temperature with an accuracy of ±0.5°C and has a repeatability of ±1°C. Further details about the sensor specifications from the manufacturer are given in table A.1 of Appendix A.

The infrared sensor produced a circular beam that had an approximate radius of 1 cm for each 10 cm distance away from the sensor. The distance between the sensor and the targeted surface determines the size of beam on the target. The size of the beam produced increases with increased distance between the sensor and the target. Figure 4.5 shows the target beam size of the infrared sensor as it changes with the measuring distance between the sensor and the targeted surface. During the experiment, the sensor beam was concentrated on the center of the soil surface whose temperature was to be measured. A laser pen was attached to the sensor which accurately targeted the center of the soil surface.
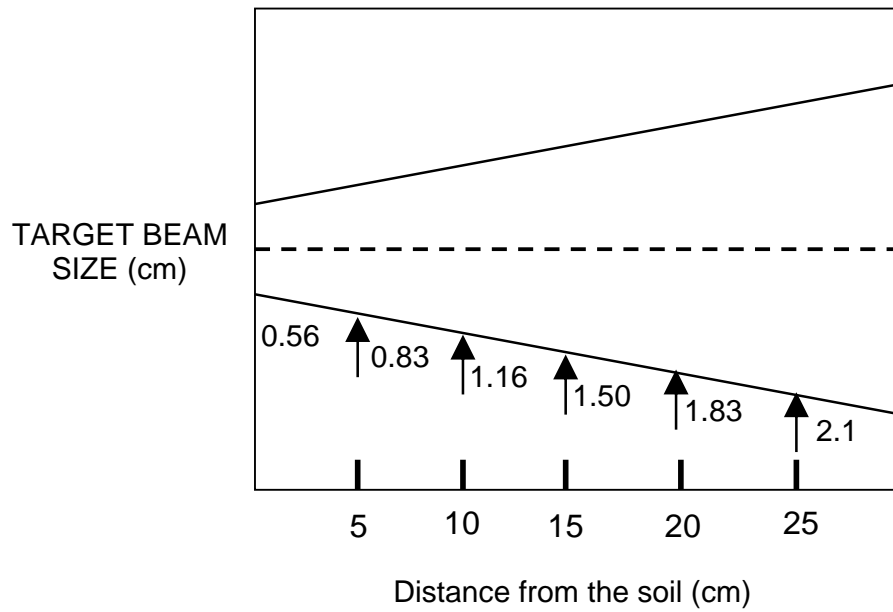
Figure 4.5 Target beam size change with distance

The sensor output was connected to the data logger through a differential input channel. The sensor input was connected to the power supply provided from the data logger which supplied 5 Volts. Figure 4.6 shows the schematic wiring diagram of the sensor.
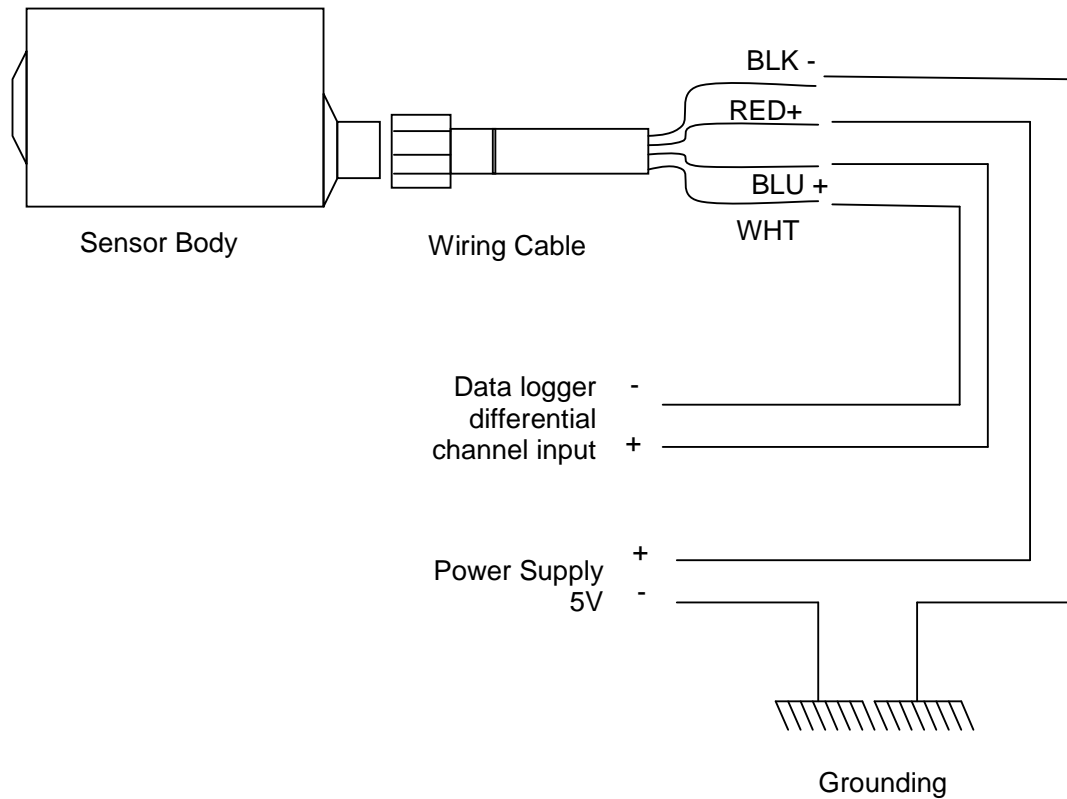
Figure 4.6 Wiring schematic of the OS43 infrared transducer

4.8.1 Indoor testing and calibration of the infrared sensor

For the purpose of calibration, the sensor was clamped above a water bath and targeted toward the center of the water surface. Two thermocouples were located on the water surface. Each thermocouple was connected to a single-ended channel of the data logger. The average value of thermocouples was calculated by summing the three voltage outputs and dividing by their number. Cold water was poured in a beaker and then the heating process was initialized. As the water temperature increased with time, the data logger kept reading measurements of the average temperature of the water surface (T_{aw}) and sensor's output in mV (Vo). A calibration equation was generated using linear regression analysis using a spread sheet program (Excel, Microsoft, 2003).

49

Figure 4.7 Indoor calibration of the thermal infrared sensor

The generated calibration model for the sensor was

$$Vo = 1.84T_{aw} + 14.22 \qquad , \qquad (4.8)$$

where:

T_{aw} : water bath surface temperature [^{o}C], and

Vo : output voltage of the thermal infrared sensor [mV].

4.8.2 Outdoor testing and calibration of the infrared sensor

Preliminary outdoor tests of the sensor showed that the sensor measurements of soil surface temperature were affected by the sensor's body temperature (T_{sens}), which in turn was affected by ambient air temperature. For illustration, for the same soil surface temperature, the sensor temperature measurements varied at different ambient temperatures. The effect appears significant at high ambient temperatures or very low ambient temperatures. Therefore, the generated calibration equation from

indoor testing would not provide accurate soil surface temperature measurements due to the effect of the sensor body temperature (T_{sens}) on measurements of the sensor when used at outdoor conditions. To overcome this problem, a thermocouple was attached to the sensor body (figure 4.8) to measure its body temperature variation (T_{sens}) during the experiment. The effect of the sensor body temperature (T_{sens}) is considered to be an error, which affects the sensor accuracy. Using linear regression analysis allows calculation of the size of error exposed from the change of sensor temperature. This will enable the researcher to reduce error and to indicate the correct surface temperature measured by the infrared sensor.
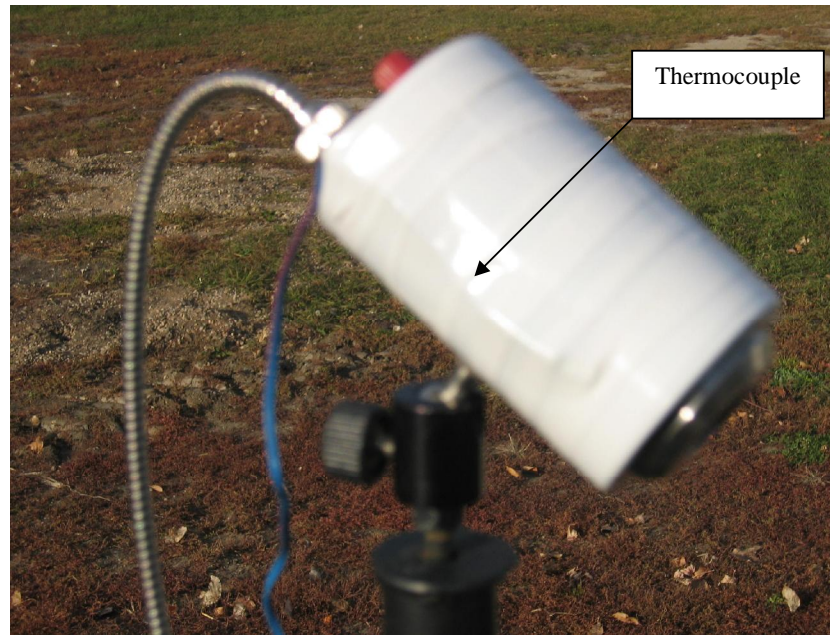
Figure 4.8 Thermocouple attached to sensor body

Three replications were used for the purpose of sensor calibration. In each replication soil surface temperature (T_s) measured by thermocouples, sensor body temperature (T_{sens}) measured by a thermocouple, soil surface temperature (T_{ir}) measured with the thermal infrared sensor, Td, RH, SR,WS, and soil moisture content (from the change of soil weight as soil dries) were recorded as the soil dried naturally during the day. These replications were taken for compacted clay soil, compacted and non-compacted sandy soil. Shortly after initiation, the infrared sensor was damaged due to the high ambient temperature changes and rain. Figure 5.10 shows the error as a function of the sensor temperature. Linear regression analysis using a spreadsheet program (Excel, Microsoft, 2003) was used for data analysis and to develop a model of the corrected soil surface temperature as measured by the infrared sensor.

4.9 Data collection

All experimental instruments were installed on the location previously mentioned. The instruments used in the experiment were infrared sensor, weather station, sensor holder, support and carrying plate and other measurement sensors. On every experiment day, the weight of dry soil was measured and the water added to create 20% soil moisture content was calculated using methods mentioned in sections 4.5 and 4.7. Prior to starting the experiment, the soil sample container was put on the carrying plate. Two thermocouples were installed in the center of the soil surface for measuring soil surface temperature (T_s) as shown in figure 4.9. The infrared sensor and the thermocouples were connected to the data logger. With the aid of a laser pen, the sensor was fixed on the holder and targeted towards the center of the soil surface. Furthermore, the weather station data logger was initialised by deleting all previous data from its memory to ensure that there was enough memory space for the new collected data. It was important to synchronize both data loggers by setting the internal clock so that both data loggers had the same time to a precision of few seconds. Then, the measurement and data collection processes were initiated and left working from nearly 10:00 A.M till after 8:00 P.M. Once the experiment was stopped, the collected data were downloaded from each data logger and saved in one file. Recorded data included soil surface temperature (T_s) measured using thermocouples inserted in the soil surface; air temperature (T_a), relative humidity (RH), solar radiation (SR), wind speed (WS) measured using the weather station; infrared sensor output voltage (Vo) (only for three replications); sensor's body temperature (T_{sens}) (only for three replications); and soil weight (w_m) as it changed. The soil moisture content (SMC) was then calculated using equation (4.9). The complete experiment setup is shown in figure 4.10.

$$SMC = \frac{w_m - w_d}{w_t} \, x100\%$$

(4.9)

where:

SMC = soil moisture content [%],

w_m = measured weight of soil during the experiment [kg],

w_d = dry weight of soil [kg], and

w_t = initial total weight of wet soil [kg].
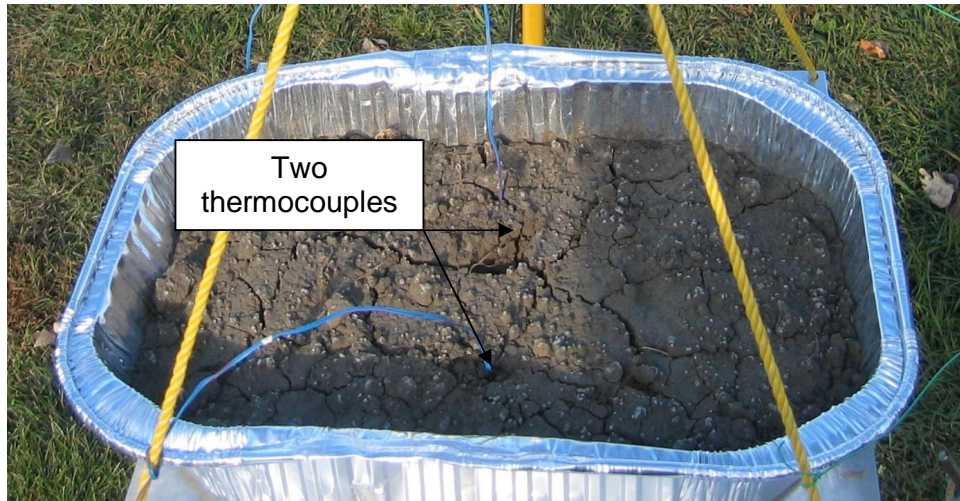
Figure 4.9 Thermocouples installed in the soil
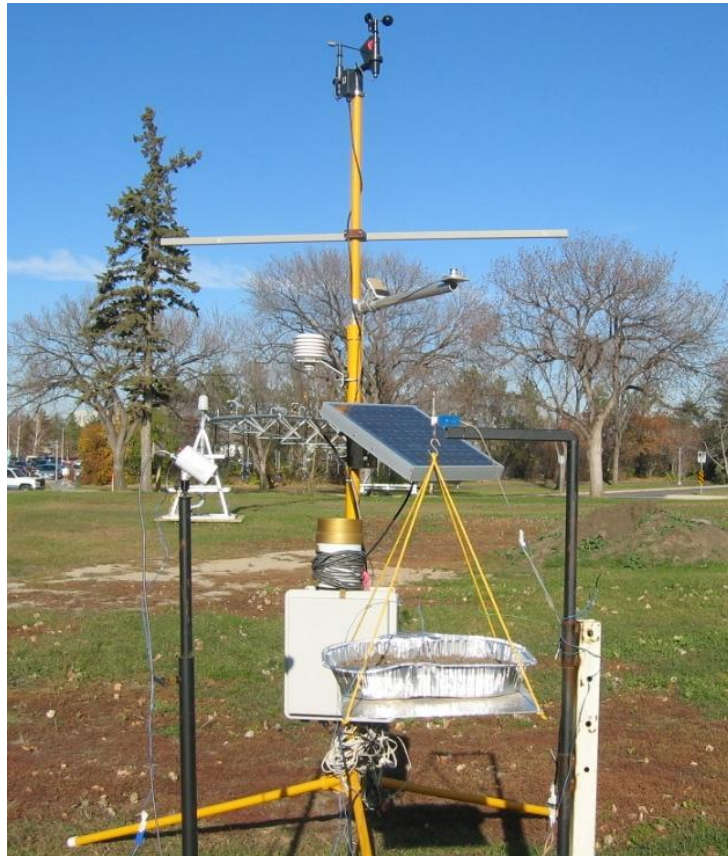
Figure 4.10 The complete experimental setup

4.10 Data analysis

The collected data (measurements) for each soil type and configuration were saved in a spreadsheet file preparing them for analysis. The measured variables were recorded at a sampling rate of 1 sample per 10 seconds. Unwanted noise occurred within the measurements due to the high sampling rate of measured variables. To solve this problem, measurements were averaged to every minute. This procedure reduced the noise to an acceptable level and the effect of noise was eliminated.

For each soil type (sand/clay), and configuration (compacted/non-compacted), three replications were used. Replications for the same soil type and configuration were then grouped together. After that, the data were randomized prior to dividing them

into the calibration and validation sets to ensure that each set was representative of the entire range of the measurements. Each replication represented the data that were collected in a day from 10:00 A.M until 8:00 P.M. Measurements were averaged to reduce noise. Data are provided in Appendix F.

4.11 Generation of multiple linear model

For the generation of the calibration models for predicting soil moisture content, SAS® (SAS Version 8, SAS Institute Inc., Cary, NC) software was used. The software is capable of performing multiple linear regression analysis using a stepwise method. Using this method, the regression equation was built of a series of multiple linear regression equations. A variable is added to the regression equation when it makes the greatest reduction in the root mean of squared errors value of the sample data. When a variable does not have a significant correlation with the dependent variable it is excluded from the regression model.

In this study, the dependent variable was soil moisture content (SMC), and the independent variables were differential temperature (T_d), solar radiation (SR), relative humidity (RH), and wind speed (WS). Because there were four independent variables used, the maximum number of independent variables (predictors) in a model is four variables while the minimum is one.

The output from SAS program showed the best four calibration models to predict the soil moisture content (SMC) for each soil type and compaction level (table5.2). It also showed the excluded models because of their low ability of prediction. The number of predictors (variables) in those four models varied from a minimum of one

to a maximum of four plus the intercept. At the end of data analysis using stepwise multiple linear regression, a summary of the output shows the regression coefficients, intercept, and R^2 values for each model that was generated. To provide a criterion for comparison between models in order to select the best one, the root mean of squared errors between the predicted and the actual values of soil moisture content were calculated for each model for both the calibration and validation data sets for each soil type and configuration. The root mean of squared errors value provides a measure of how well the predicted values fit the measured ones. The smaller value of the root mean of squared errors notes smaller differences between the actual and predicted values, and thus a higher model performance. The root mean of squared errors was calculated using the following equation:

$$RMSE = \sqrt{\frac{\sum (y - x)^2}{n - 1}} \qquad \textbf{(4.10)}$$

In equation 4.10, x is the actual measured soil moisture content (SMC) and y is the predicted one from the developed models. The variable n indicates the number of measurements (samples). The RMSE value for the calibration data was calculated and was named as RMSEC. Similarly, the RMSE value for the validation data set was also calculated and named as RMSEV.

Because the sizes of the calibration and the validation data sets were different because only 1/3 of the data was used for validation while 2/3 was used for calibration, the use of RMSE was suitable. This is because it calculates the root mean

of the sum of squared differences, which eliminates the effect of the unequal sample sizes and makes the comparison between RMSEC and RMSEV valid.

Another important value to be determined was the sample coefficient of determination (R^2). This value provides a measure of the degree of linearity between two variables or the degree of covariance between them. It is known that the addition of more variables into the regression model increases its R^2 value. The coefficient of determination (R^2) was calculated using spreadsheet software (MS-EXCEL, Microsoft Corp, 2003).

4.12 Discussion of model performance

All calibration models that were generated should be evaluated using some metrics to choose the best model. This can be done by comparing calibration (RMSE and R^2) and validation RMSE. High R^2 value is not enough of a measurement level to judge on a model performance because its value increases with the number of variables entered in the regression model. Also needed is the root mean of squared errors (RMSE) to be another criterion because it has the ability to explain the difference between the actual and predicted values of soil moisture content. The difference between RMSEC and RMSEV values for the same model should not be large. For example, if the value of RMSEC is much lower than the RMSEV, this shows that there is an over-fitting towards the calibration data set and an unacceptable fitting towards the remainder of the data (the validation data set). Therefore, this model performs well for only part of the data (the calibration data set) and performs with lower performance for the remainder of the data (the validation data set).

Furthermore, the number of variables in a model is another criterion which is used in the selection of the best model. It is advisable to select a model with a lower number of variables, to reduce cost and complexity. Some smaller models still provide comparable predictive performance similar to the large size models. This does not necessarily mean that a model with a smaller size will be selected in favor of its performance. But if there is a difference in performance between two models, small or insignificant, then it is advisable to select the smaller size model.

5. RESULTS AND DISCUSSION

5.1   Collected measurements

The graphs in Figure 5.1 through 5.4 show the change in the level of soil moisture content, air temperature, and soil surface temperature with time for replications number 2 of each soil type and configuration used in this study. Other experiment data: relative humidity, solar radiation, and wind speed are given in the tables in Appendix F where those graphs were derived. The remainder of the replications are given in Appendix B. In some replications missing data were due to problems associated with data retrieving from the data logger. There were sufficient measurements because the number of data in each replication was enough to provide a reliable description about the relation between the dependent variable, SMC, and the independent variables T_d, RH, SR, and WS. There is acceptable confidence about the number of data available to produce a calibration model that can accurately predict the soil moisture content for all soil types and configurations.

In general, the graphs from Figure 5.1 to 5.4 showed that the soil moisture content is decreased with time starting from nearly 20% soil moisture content until it reached a soil moisture content that ranged between 8-16%. All soil types and configurations showed a relatively high evaporation rate. This outcome was expected, because there was high initial moisture content ($\approx$20%) and relatively thin soil sample depth of about 6 cm.
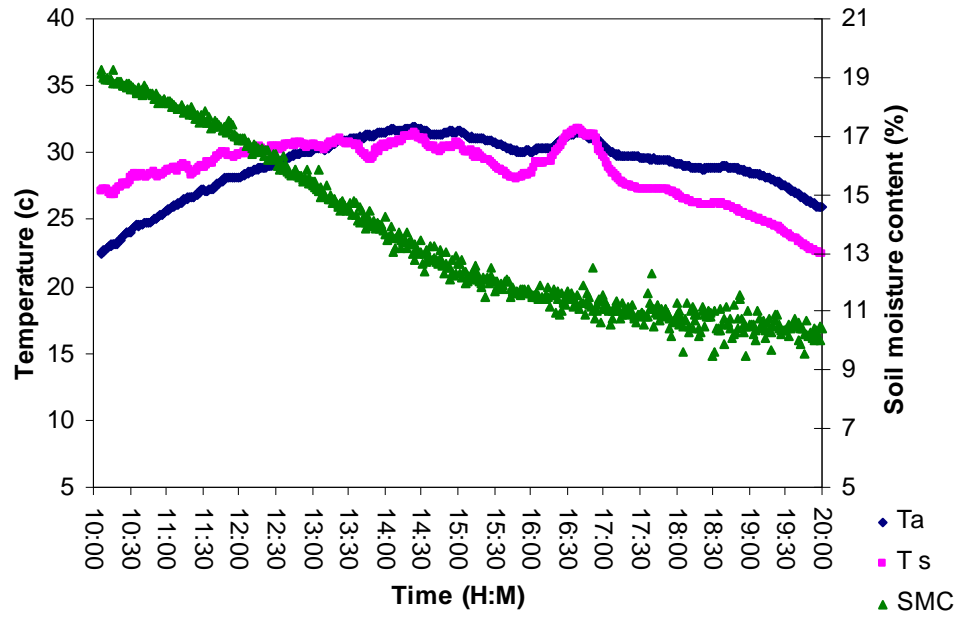
Figure 5.1 Air temperature (T_a), soil surface temperature (T_s) measured using thermocouples, and soil moisture content (SMC) versus time for replication 2 of clay compacted soil.
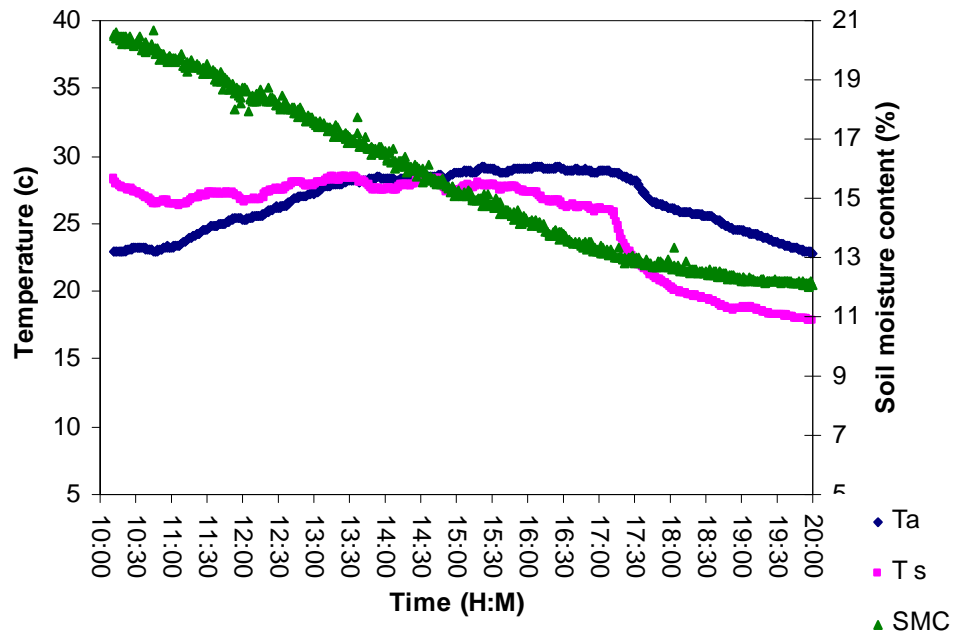
Figure 5.2 Air temperature (T_a), soil surface temperature (T_s) measured using thermocouples, and soil moisture   content (SMC) versus time for replication 2 of clay non-compacted soil
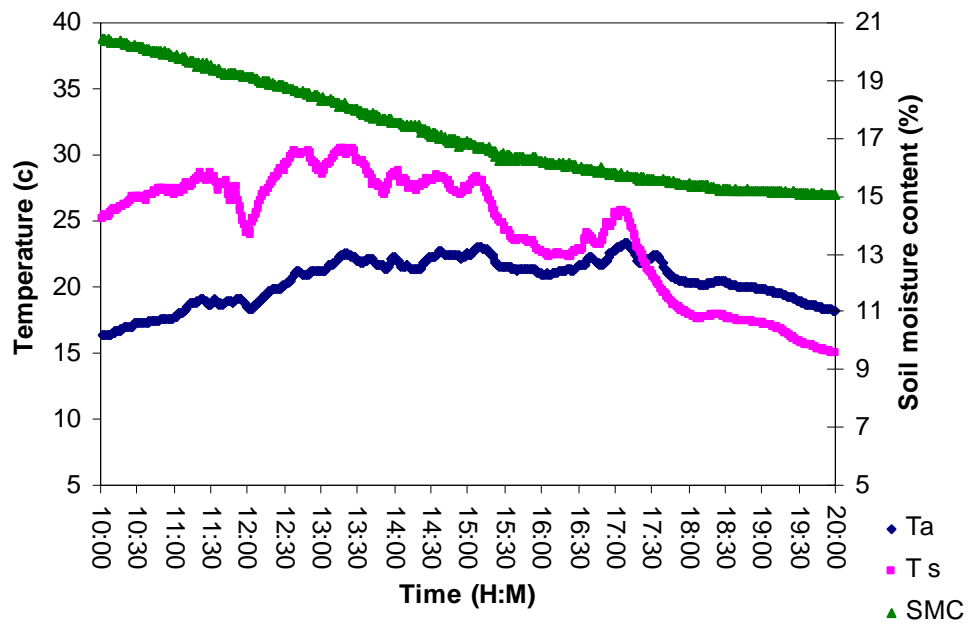
Figure 5.3 Air temperature (T$_a$), soil surface temperature (T$_s$) measured using thermocouples, and soil moisture content (SMC) versus time for replication 2 of sand compacted soil.
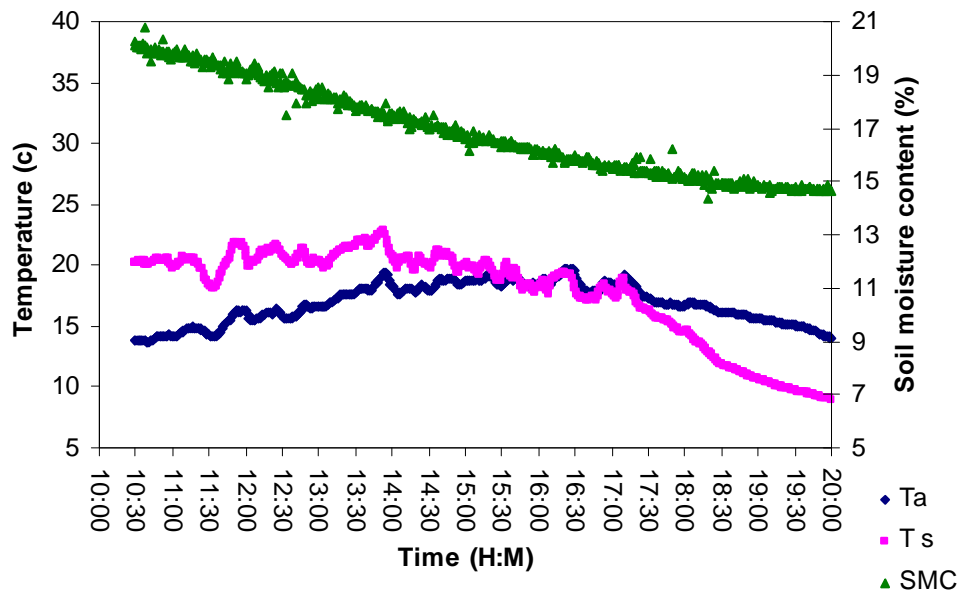
Figure 5.4 Air temperature (T$_a$), soil surface temperature (T$_s$) measured using thermocouples, and soil moisture content (SMC) versus time for replication 2 of sand non-compacted soil.

For all soil types and configurations (compacted/not compacted), the soil surface temperature was higher than the air temperature at the beginning of the experiment, and eventually both became equal at a certain time of the day, and finally the air temperature became higher at night. This was the case for all soil types and configurations except for replication 1 of compacted sandy soil, where the air temperature was always higher than the soil surface temperature during the experiment. This is believed to be due to the high air temperature for that day (replicate) compared to other days (replicates).

Figures 5.1 through 5.4 show that the rate of soil moisture loss was highest between 10:00 a.m. and 4:00 p.m. and then became low at the end. This is due the presence of high amounts of water, high solar radiation, and relatively high air temperature in the daytime compared to the evening and after most of the water had evaporated. The clay soils (compacted and non-compacted) (Figures 5.1 and 5.2) show that, the soil surface temperature (Ts) and air temperature (T_a) became equal during earlier periods of the day compared to the other soil (sand). In general, all graphs of the different soil types and configurations show a similar trend and shape. The difference between them is mainly due to the nature of the surrounding environment at the experimenting time and, secondly, due to soil type and compaction level.

5.2 Consolidated results of the collected measurements

To make a comparison between the different soil types and configurations easier, the average values of the measured variables of the three replications for each soil type and configuration were calculated and are given in table 5.1. Further clarification about the method used to produce this table is given in Appendix F. Table 5.1 shows that compacted clay soil has the highest loss of moisture content from about a maximum of 19% to 9.3 %. This is considered to be a 51% change in the level of moisture content. This outcome was expected, because the average values of air temperature (T_a), wind speed (WS), and solar radiation were the highest for compacted clay soil among other soil types and configurations (table 5.1). Furthermore, compacted clay soil had the lowest relative humidity of 36.5%. The total loss of soil moisture content of the remainder of the soil types and configurations were lower than that of the compacted clay soil; 30% for clay non-compacted soil; 33% for compacted sand soil; and 36.5% for sand non-compacted soil. Both the compacted and the non-compacted clay soils had negative average values of differential temperature (T_d); -0.1°C for compacted clay soil and -1.2°C for clay non-compacted soil. On the other hand, both the compacted and the non-compacted sandy soils had positive average values of differential temperature (T_d); 1.6°C for compacted sandy soil and 0.3°C for non-compacted sandy soil.

Table 5.1 Average values of measured variables of three replicates for each soil type and configuration

Variable	Statistic	Clay compacted	Clay non-compacted	Sand compacted	Sand non-compacted
$SMC^{†}$	Averaged maximums	19.0	19.6	19.0	20.0
	Averaged minimums	9.3	13.9	12.7	12.7
$T_d{}^{‡}$	Average	-0.1	-1.2	1.6	0.3
$Ts^{‡}$	Average	26.0	22.4	25.2	21.1
$Ta^{‡}$	Average	26.0	23.6	23.6	20.8
$RH^{ψ}$	Average	36.5	46.2	39.7	38.9
$WS^{ψ}$	Average	2.7	1.9	1.5	1.9
$SR^{¥}$	Average	957.7	739.6	898.9	921.5

[†]Soil moisture content (SMC) values are in percentage
[‡]Differential temperature (Td), soil surface temperature (Ts), and air temperature (Ta) are in $°C$
[ᵁ]Relative humidity (RH) values are in percentage
[ψ]Wind speed (WS) values are in m/s
[¥]Solar radiation (SR) values are in $w.m^{-2}$

5.3   Development of regression models

Using stepwise linear multiple regression analysis, a total of 16 regression models were generated for all soil types and configurations (table 5.2). Calibration data sets were used in the analysis process. For each soil type and configuration, four models were generated and ranked by the coefficient of determination value R^2 (table 5.2). All models of the same size of all soil types and configurations showed great consistency. The variables for those models were T_d for model 1; T_d and RH for model 2; T_d, RH, and SR for model 3; and T_d, RH, SR, and WS for Model 4. Those

65

variables were ranked within each model based on the level of effect each variable

had on the dependent variable (soil moisture content).

Table 5.2 Multiple linear regression parameters

Soil type & configuration	Model	Regression coefficients					R^2
		constant	T_d	RH	SR	WS	
CLAY– COMPACTED	MLR1	13.064	0.99	-	-	-	0.68
	MLR2	10.499	0.88	0.07	-	-	0.71
	MLR3	8.795	0.707	0.091	0.001	-	0.72
	MLR4	10.074	0.704	0.078	0.001	-0.335	0.73
CLAY NON- COMPACTED	MLR1	16.875	0.605	-	-	-	0.68
	MLR2	15.226	0.579	0.035	-	-	0.70
	MLR3	12.836	0.446	0.067	0.001	-	0.72
	MLR4	13.281	0.451	0.066	0.001	-0.219	0.72
SAND COMPACTED	MLR1	14.525	0.432	-	-	-	0.62
	MLR2	9.680	0.361	0.125	-	-	0.86
	MLR3	10.503	0.418	0.114	-0.001	-	0.86
	MLR4	11.102	0.416	0.114	-0.001	-0.413	0.86
SAND NON- COMPACTED	MLR1	15.210	0.515	-	-	-	0.59
	MLR2	10.283	0.397	0.128	-	-	0.80
	MLR3	8.591	0.249	0.147	0.001	-	0.82
	MLR4	8.023	0.252	0.146	0.001	0.349	0.83

MLR1 denotes multiple linear regression model number 1
MLR2 denotes multiple linear regression model number 2
MLR3 denotes multiple linear regression model number 3
MLR4 denotes multiple linear regression model number 4

Table 5.2 shows the regression coefficients of each variable in the developed models

for each soil type and configuration. Differential temperature (T_d) had the greatest

effect on the prediction of soil moisture content (SMC). Relative humidity (RH)

came second, solar radiation (SR) third, and finally wind speed (WS). T_d values for all models of the same size (same number of variables) of different soil type and compaction level were consistent. The value of T_d coefficient was positive for all models and ranged from a minimum of 0.249 for Model 4 of sand non-compacted soil to a maximum of 0.990 for Model 1 of compacted clay soil. For the same soil type and configuration, the value of T_d coefficient was the highest for models MLR1 having only one variable, T_d, and this value decreased in the larger models. This decrease was due to the addition of more variables to the regression model. Those new added variables shared the effect with T_d. The T_d coefficient values are higher in clay soils than in sandy soils, which means that T_d has a greater effect in clay soils than in sandy soils. This can be seen from the values of R^2 for MLR1 between clay soils and sandy soils; the values are higher for clay soils. On the other hand, the relative humidity (RH) variable has more of an effect in sandy soils. This effect can be seen in the increase in the value of R^2 for MLR2 compared to the slight increase in this value in MLR2 of clay soils. Regarding the effect of solar radiation (SR), it was observed that the value of SR coefficient was small and posed relatively lower effect than those of relative humidity (RH) and temperature difference (T_d) but higher than the wind speed (WS) variable. A phenomenon, which deserves to be considered, is the values of SR coefficients in MLR3 and MLR4 for compacted sandy soil. These values were negative, whereas they were positive in all other models of other soil types and configurations.

The values of R^2 of all soil types and configurations and all models ranged from a minimum of 0.59 in MLR1 of non-compacted sandy soil to a maximum of 0.86 in MLR2, MLR3 and MLR4 of compacted sandy soil. In general, the values of R^2 in

the calibration models of sandy soil were higher than those of clay soils. While the value of R^2 does not exceed 0.73 in the largest size model (MLR4) for compacted clay soil and 0.72, for non-compacted clay soil, it reaches 0.86,for compacted sandy soil, and 0.83 for non-compacted sandy soil for the same model size. It should also be noted that all wind speed (WS) coefficients of Model 4 for all soil types and configurations were negative, except one which was positive in non compacted sandy soil (table5.2). The negative sign of the wind speed coefficient indicates that, as wind speed goes higher, the moisture content present in the soil goes lower. This was expected since high wind speed increases the rate of loss of moisture from the soil surface and consequently reduces the amount of moisture present in the soil.

5.3.1   Compacted clay soil regression model

Variables and regression coefficients used to predict soil moisture content (SMC) of compacted clay soil are given in table 5.2. The statistical parameters, RMSEC and the R^2 of the calibration data set are given in table 5.3. The compacted clay soil models generated using the calibration data set showed relatively good R^2 values ranging from minimum of 0.68 to a maximum of 0.73. The increase of the value of R^2 with the number of variables added to the regression models was minimal from Model 1 to Model 2, but gradual from Model 2 to Model 4. The larger regression model sizes were associated with higher R^2 values. The RMSEC values varied from 1.61 for the four-variable model to 1.77 with the single-variable model as shown in table 5.3. In general, the developed models explained approximately 68% to 73 % of the calibration data set.

The R^2 and RMSEV values for the validation data set were also calculated and shown in table 5.3. The comparison between the statistical parameters of the calibration data set and the validation set shows that the R^2 value of the latter was higher and with lower RMSEV values. Again, there was a minimal increase in the R^2 value from the single-variable model to the two-variable model, and a gradual increase from Model 2 to the four-variable model. The R^2 values ranged from a minimum of 0.69 to a maximum of 0.74, with RMSEV values ranging from 1.55 to 1.72. Table 5.3 shows that the RMSEV values decreased with the increase of R^2 values. The lowest validation RMSE value occurred for the highest coefficient of determination. This was the expected outcome, because a larger model with more variables has a higher capability of detecting the variation and minimizing it.

Results showed that the RMSEC and RMSEV values for all the models were close. This indicates that both the calibration and validation data sets were well representative of the entire range of the data and that there was no significant over-fitting during the training process. Model 3 (MLR3) was selected as the appropriate model for prediction. It has relatively good R^2, as well as low calibration and validation RMSE values. It is the best predictive model, favoring reduction in size of the model to the smaller contribution of larger models in minimizing the RMSE value. In addition, there was no significant difference between the calibration RMSEC and validation RMSEV.

Table 5.3 Calibration and validation results of compacted clay soil models

Statistic	Regression models			
Calibration	MLR1	MLR2	MLR3	MLR4
R^2	0.68	0.71	0.72	0.73
RMSEC	1.77	1.68	1.64	1.61
Validation				
R^2	0.69	0.72	0.73	0.74
RMSEV	1.72	1.62	1.59	1.55

A plot of the predicted versus actual SMC values of the selected model showed a good fit over the whole range of validation data as shown in figure 5.5 below. For the same model, the R^2 and RMSE values were higher and lower respectively for the validation data sets than those of the calibration data sets. The figure shows that there is a partial over-estimating in predicted soil moisture content values below 10%. The predicted SMC values were slightly higher than the actual ones. Model 3 contains three variables: differential temperature (T_s), relative humidity (RH), and solar radiation (SR).

Figure 5.5 Predicted versus actual soil moisture (SMC) for the three-variable model
(MLR3)

5.3.2   Non-compacted clay soil regression model

Variables and regression coefficients used to predict soil moisture content (SMC) of

non compacted clay soil are given in table 5.2. The RMSEC and R^2 values that will

be used to evaluate the performance of the models are given in table 5.4. Stepwise

multiple linear regression analysis of the calibration data set of this soil showed

relatively similar R^2 values similar to those of compacted clay soil. The coefficient of

determination R^2 values ranged from a minimum of 0.68 to a maximum of 0.72.

RMSEC values of this soil were lower than those of compacted clay soil. Model 3

and model 4 had equal R^2, and RMSEC values of 0.72 and 1.14 respectively. This

indicates that the addition of more variables did not significantly improve the

prediction ability of Model 4. This could be due the minimal contribution of the

added variable on the effect on the soil moisture content in this soil type and

configuration. RMSEC values ranged from a maximum of 1.22 for a single-variable model to a minimum of 1.14 for three- and four-variable models. As expected, the coefficient of determination (R^2) value increased with the addition of more variables into the regression model. Thus, MLR4 has the highest coefficient of determination value while MLR1 has the lowest.

The performance of the generated models was tested using the validation data set. R^2 and RMSEV values of the validation data set are given in table 5.6. When tested with the validation data set, models produced higher R^2 values than those of the calibration data set but had lower RMSEV values. This indicates that the models had performed slightly better with the validation data set. R^2 values increased from 0.72 for a single-variable model to 0.78 for a four-variable model. Conversely, the RMSEV value decreased from 1.15 to 1.03.

The best non-compacted clay soil model was the three-variable model with a calibration R^2 value of 0.72, validation R^2 value of 0.77, RMSEC of 1.14 and RMSEV of 1.04.

Table 5.4 Calibration and validation results of non-compacted clay soil models

Statistic	Regression models			
Calibration	MLR1	MLR2	MLR3	MLR4
R^2	0.68	0.70	0.72	0.72
RMSEC	1.22	1.18	1.14	1.14
Validation				
R^2	0.72	0.75	0.77	0.78
RMSEV	1.15	1.10	1.04	1.03

A plot of the measured versus predicted soil moisture content using the selected model MLR3 is given in figure 5.6. The graph shows acceptable prediction ability of this model. However, the selected model (Model 3) tends to overestimate the soil moisture content in the ranges between 10% and 15%. Model 3 contains three prediction variables-differential temperature (T_d), relative humidity (RH), and solar radiation (SR).

Figure 5.6 Predicted versus actual soil moisture (SMC) for the three-variable model (MLR3)

5.3.3 Compacted sandy soil regression model

Variables and regression coefficients used to predict soil moisture content (SMC) of compacted sandy soil are given in table 5.2. The results of the calibration data and performance analysis showed high R^2 values and low RMSEC values. The lowest R^2 value was 0.62 which occurred for the single-variable model (MLR1). It is important to mention that the R^2 value was kept equal to about 0.86 for Models 2, 3, and 4 and was not affected by the addition of more variables to the regression models. This result was not expected, because the addition of more variables should increase the R^2 value. Model 2 had the lowest RMSEC value of 0.99 while Model 1 (MLR1) had the highest of 1.63. There is no doubt that the best model is Model 2 because it had a high R^2 value of 0.86 and at the same time very low RMSEC and RMSEV values.

The R^2 and RMSEV values of the validation data set are given in table 5.5. In general, the validation data set had slightly lower R^2 values than those of the calibration data set and higher RMSEV values. The highest R^2 value was 0.86 which occurred for Model 2 (MLR2) and the lowest was 0.64 for Model 1 (MLR1). Calculation of RMSEV for all models using the validation data set showed the lowest RMSEV value of 1.00 when using Model 2 for prediction, and the highest of 1.63 when MLR1 was used.

MLR2 had the highest calibration R^2 value, equal to those of MLR3 and MLR4 and the highest validation R^2. It also had the lowest calibration and validation RMSE values. This model combined two advantages: the small size (few numbers of variables) and high prediction performance.

Table 5.5 Calibration and validation results of compacted sandy soil models

Statistic	Regression models			
Calibration	MLR1	MLR2	MLR3	MLR4
R^2	0.62	0.86	0.86	0.86
RMSEC	1.63	0.99	1.01	1.01
Validation				
R^2	0.64	0.86	0.85	0.85
RMSEV	1.63	1.00	1.03	1.04

A plot of the predicted versus measured SMC values of the selected model showed a good fit at some moisture content ranges and overestimated at others over the whole range of validation data as shown in figure 5.7. The figure shows that there is a partial over-estimating in predicted soil moisture content values below 13% and above 19 %. The predicted SMC values were slightly higher than the actual ones.
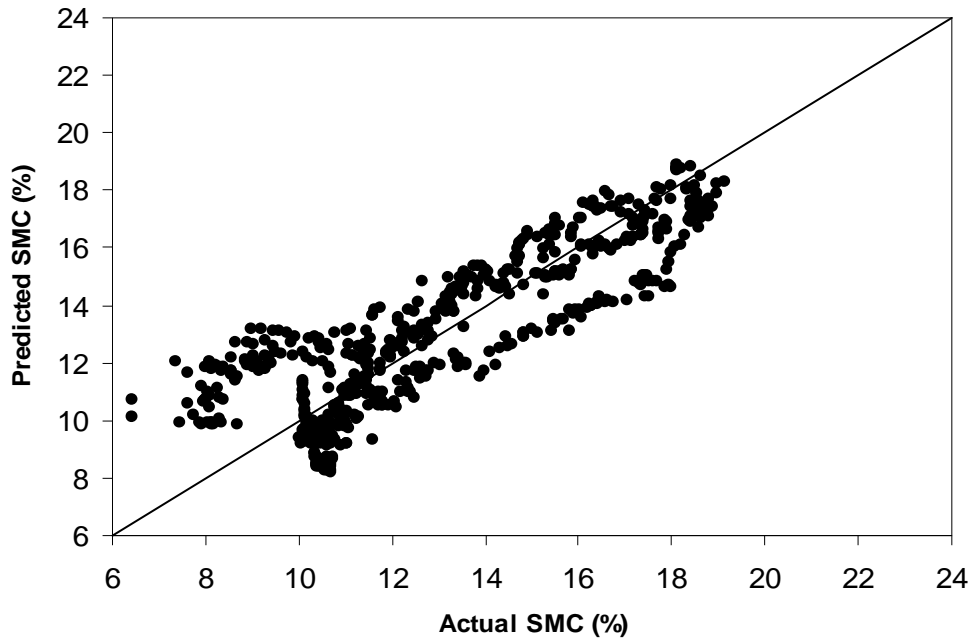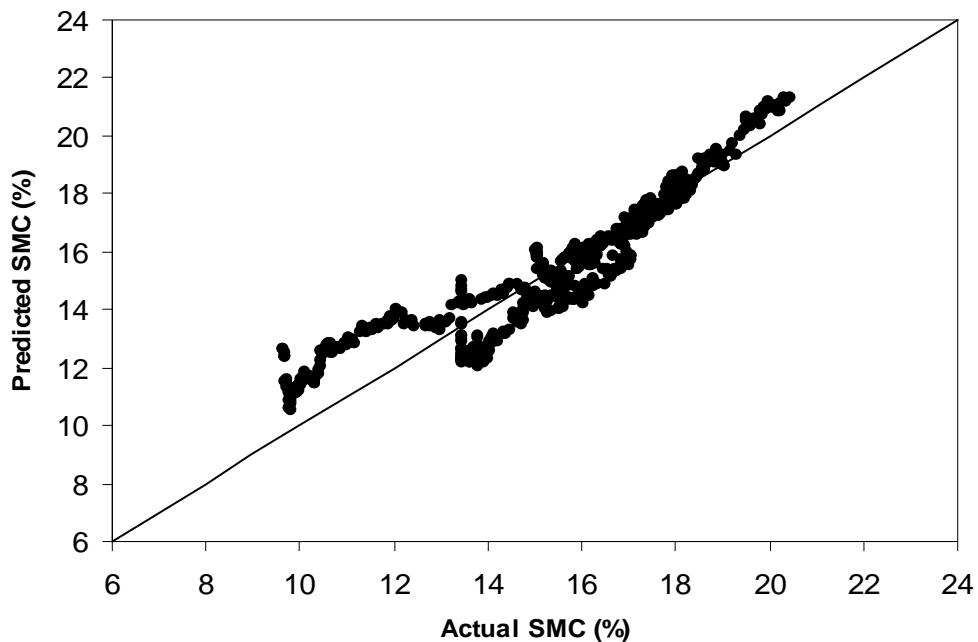

Figure 5.7 Predicted versus actual soil moisture (SMC) for the two-variable model (MLR2)

5.3.4 Non -compacted sandy soil regression model

Some models and the corresponding regression coefficients used to predict soil moisture content (SMC) of non-compacted sandy soil are given in table 5.2. In general, the results of calibration data and performance analysis showed good R^2 values and low RMSEC values. This performance was comparable to models developed for clay soils, but was not as high as for compacted sandy soil. The highest R^2 value was 0.83 which occurred for the four-variable model (MLR4), and the lowest was 0.59 which occurred for the single-variable model (MLR1). There was a significant increase of R^2 value from Model 1 to Model 2, but then the increase was minimal. As was expected, the addition of more variables to the regression model caused an increased R^2 value. Conversely, the RMSEC value decreased with the addition of more variables to the regression model. The lowest RMSEC value was 1.04 which occurred for the four-variable model, and the highest was 1.59 which occurred for the single-variable model.

The generated models, using the calibration data set, were tested using the validation data set. This procedure provides a tool to test the generated model for prediction performance and generality. R^2 and RMSEV values of the validation data set are given in table 5.6. In general, the validation data set had slightly lower R^2 values than those of the calibration data set and higher RMSEV values. The highest R^2 value was 0.81 which occurred for Model 3 (MLR3) and model 4 (MLR4), and the lowest was 0.59 which occurred for Model 1 (MLR1). The increase of R^2 with the addition of more variables to the regression models was drastic from Model 1 to Model 2. R^2 value increased approximately by 26 %. R^2 value increased slightly from Model 2 to

Model 3 and stayed the same for Model 4. The lowest RMSEV value was 1.07 which occurred for Models 3 and 4, and the highest was 1.59 which occurred for Model 1.

The selection of the best model depends on the performance of the model and the number of variables it contains. A high R^2 value and low RMSEC and RMSEV values indicate higher model performance. Another criterion is the size of the model. Smaller models, having fewer variables, is favored over a large model size with slightly better performance. Having that in mind and from the results, Model 4 cannot be the best model because Model 3, with fewer variables, performed similarly to Model 4. Therefore, Model 3 (MLR3) was selected as the best model for prediction. It has relatively good R^2 as well as low calibration and validation RMSE values. It is the best predictive model favoring reduction in size of the model compared to the smaller contribution of larger models in minimizing the RMSE value as in Model 4 mentioned earlier.

Table5.6 Calibration and validation results of non-compacted sandy soil models

Statistic	Regression models			
Calibration	MLR1	MLR2	MLR3	MLR4
R^2	0.59	0.80	0.82	0.83
RMSEC	1.59	1.11	1.05	1.04
Validation				
R^2	0.59	0.79	0.81	0.81
RMSEV	1.58	1.12	1.07	1.07

A plot of the predicted versus actual SMC values of the selected model showed a relatively high prediction performance for moisture content from 13 % to 20 %. On the other hand, the model tended to overestimate the soil moisture content below 13

%. The plot is shown in figure 5.8. Model 3 contained three variables: differential temperature (T_d), relative humidity (RH), and solar radiation (SR).

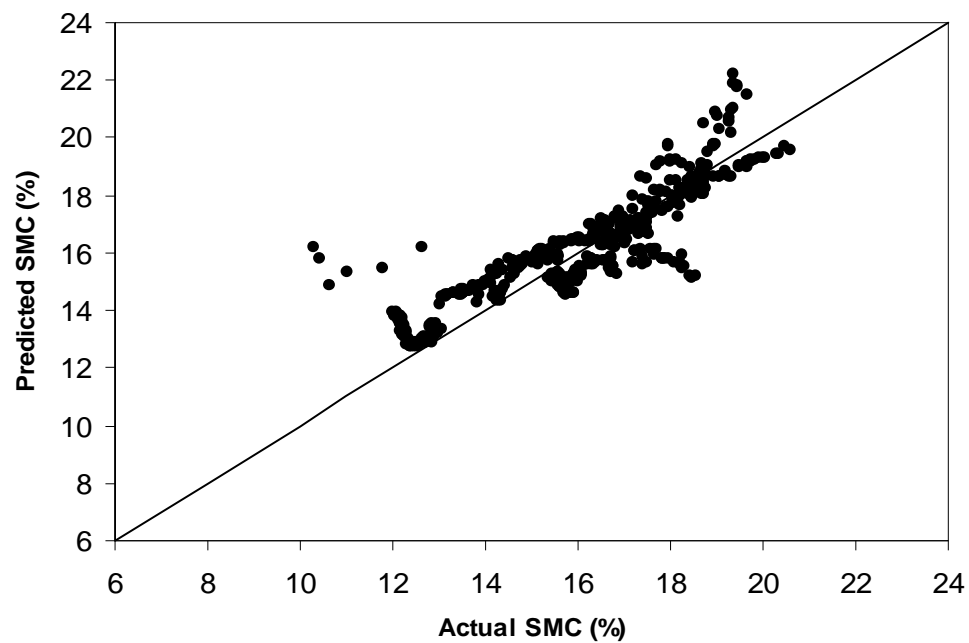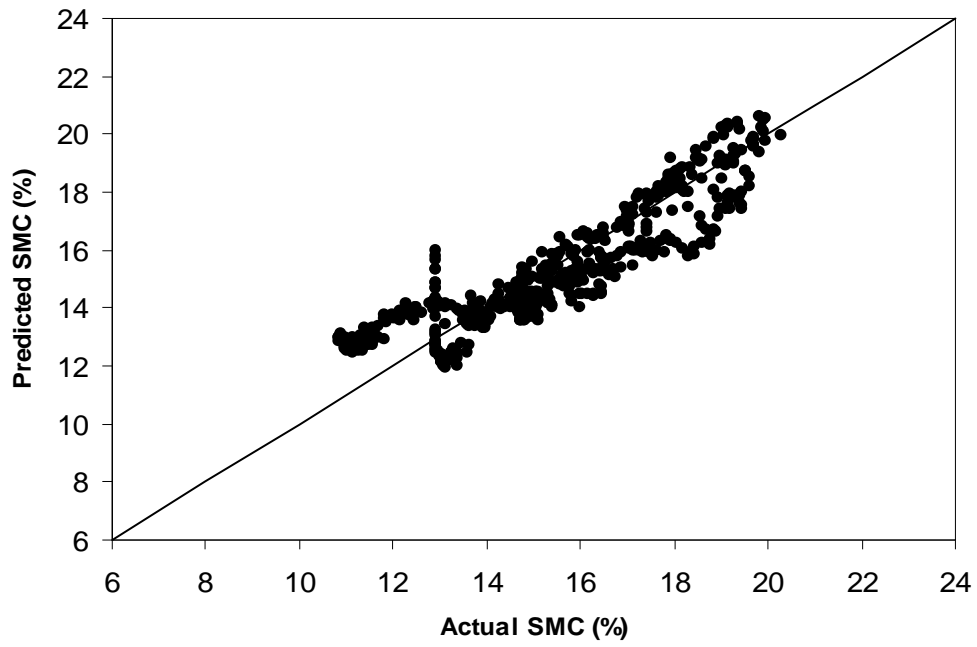Figure 5.8 Predicted versus actual soil moisture (SMC) for the three-variable model (MLR3)

5.4 Sensor calibration and testing

Figure 5.9 shows one replication of the measurements of soil surface temperature (T_s), sensor body temperature (T_{sens}), and soil surface temperature as measured by the thermal infrared sensor (T_{ir}) as a function of time. The other two replications are shown in Appendix B. From the figure it can be seen that the sensor body temperature (T_{sens}) changed with the same pattern as the change in soil surface temperature measured by the thermocouple (T_s), and the soil surface temperature measured by the sensor (T_{ir}). This result was expected since the sensor was exposed to the same ambient temperature and environment.
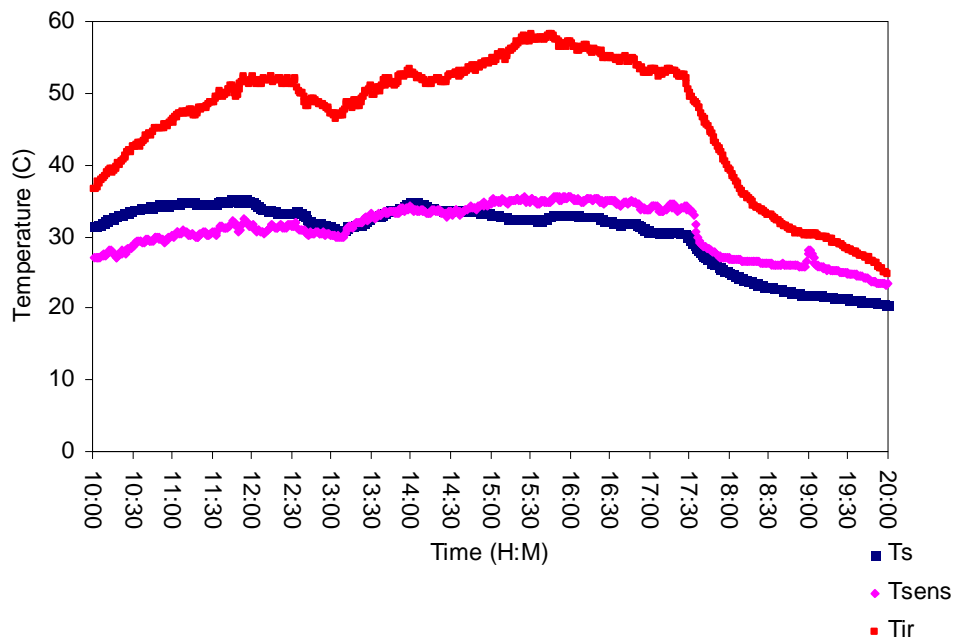
Figure 5.9 Soil surface temperature measured by thermocouple (T_s), soil surface temperature measured by the sensor (T_{ir}), sensor body temperature (T_{sens}) for first replication.

5.4.1 Effect of the change of sensor body temperature on the sensor accuracy

Figure 5.10 shows the effect of sensor body temperature on the accuracy of the measured soil surface temperature by the sensor (T_{ir}). When the sensor body temperature increases above or decreases below a certain temperature range (approximately between 21°C and 22°C), the difference between T_s and T_{ir} also increases. The difference reached the maximum value of 25.7°C when the sensor body temperature reached (35.4°C). This is considered to be a large difference which negatively affects the accuracy of the soil surface temperature measurements taken by the thermal infrared sensor.

5.4.2 The corrected T_{ir} value

Figure 5.10 shows the temperature difference as a function of the sensor body temperature. The temperature difference equals the soil surface temperature measured by thermocouples (Ts) minus the soil surface temperature measured by the sensor (T_{ir}) for the three replications used (see equation 5.2). Linear regression analysis using a spreadsheet program (Excel, Microsoft, 2003) was used for data analysis and to develop a model which correlated the temperature difference to the sensor body temperature.
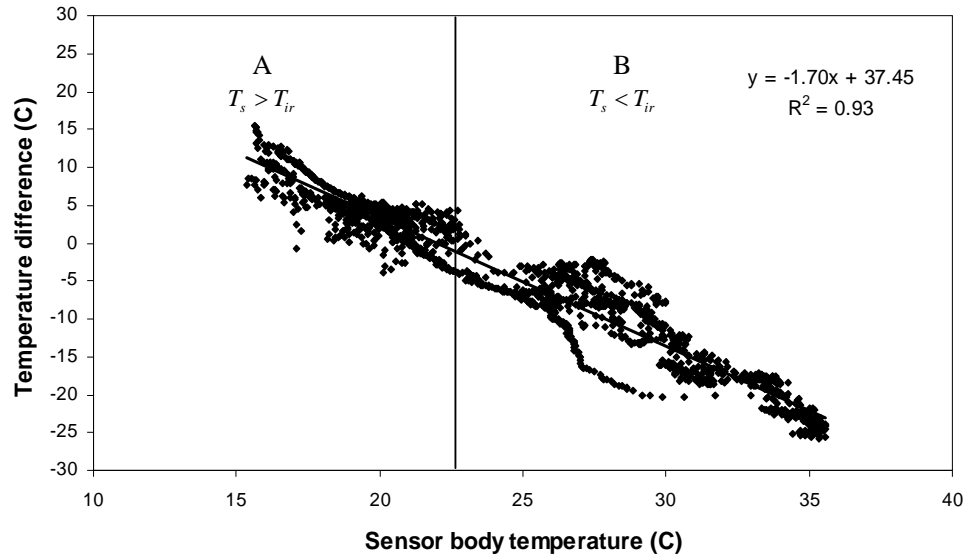
Figure 5.10 Temperature difference between soil temperature measured with thermocouples, T_s, and the infrared sensor, T_{ir}, as a function of the sensor body temperature.

Applying linear regression analysis using a spreadsheet program (Excel, Microsoft, 2003) to the data resulted in a linear equation which correlates the measurement error to the sensor body temperature .The developed equation is as follows:

$$E = -1.7 T_{sens} + 37.5 \,, \tag{5.1}$$

where

$$E = T_s - T_{ir} \qquad , \tag{5.2}$$

E = temperature difference [°C],

T_s = soil surface temperature measured using thermocouples [°C] and

T_{ir} = soil surface temperature measured using the thermal infrared sensor [°C].

The minimum level of error occurs when E is equal to zero as shown in figure 5.10. The temperature of the sensor body (T_{sens}) at which the error is zero can be determined by solving equation 5.1 for T_{sens} when $E=0$.

$$T_{sens} = \frac{37.5}{1.7} = 22.1C° \tag{5.3}$$

In figure 5.10, a vertical line is drawn perpendicular to the x-axis and crosses it at the sensor body temperature ($T_{sens}=22.1C°$) where E is zero. The line separates the chart area into two regions namely region A and region B. In region A, $T_{s} > T_{ir}$ and in region B, $T_{s} < T_{ir}$. This indicates that the measured soil surface temperature using the thermal infrared sensor (T_{ir}) increases with the increase of the sensor body temperature and vice versa.

The corrected soil surface temperature measured by the sensor can be calculated by rearranging equation 5.1 to be:

$$T_{ir}(corrected) = T_{ir} - 1.7Tsens + 37.5 \quad . \tag{5.4}$$

5.4.3 Estimating the soil moisture content using thermal infrared sensor

The corrected value of T_{ir} can be calculated using equation 5.4 and is used to calculate the soil-minus-air temperature (T_{d}) value which was used as a variable in the developed models for each soil type and configuration. The previous generated calibration models were developed using the soil surface temperature (T_{s}) measured by the thermocouples.

Figures 5.11 and 5.12 show the actual soil moisture content measurements versus the predicted SMC measurements using thermocouples and the predicted SMC measurements using the infrared sensor for MLR2 of sand compacted soil and MLR3 of sand non-compacted soil, respectively. No measurements were collected for clay soils with the infrared sensor because the infrared sensor got damaged before more measurements could be done on clay soils. The figures show good compatibility between the soil moisture measurements taken by thermocouples and the infrared sensor.
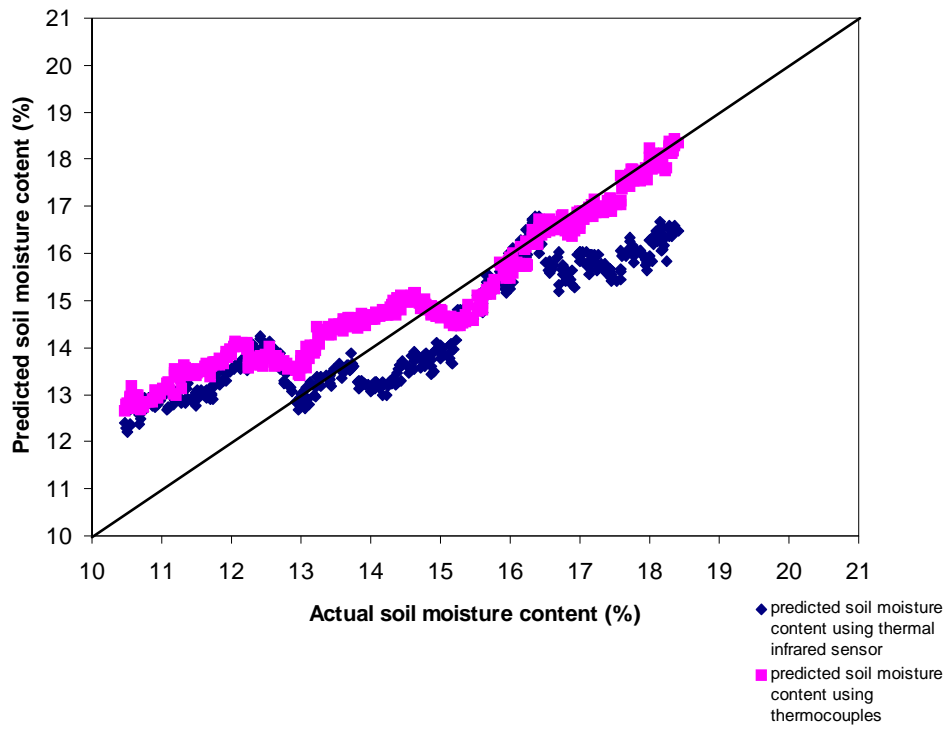
Figure 5.11 Actual versus predicted SMC using thermocouple and the infrared sensor for MLR2 of sand compacted soil.
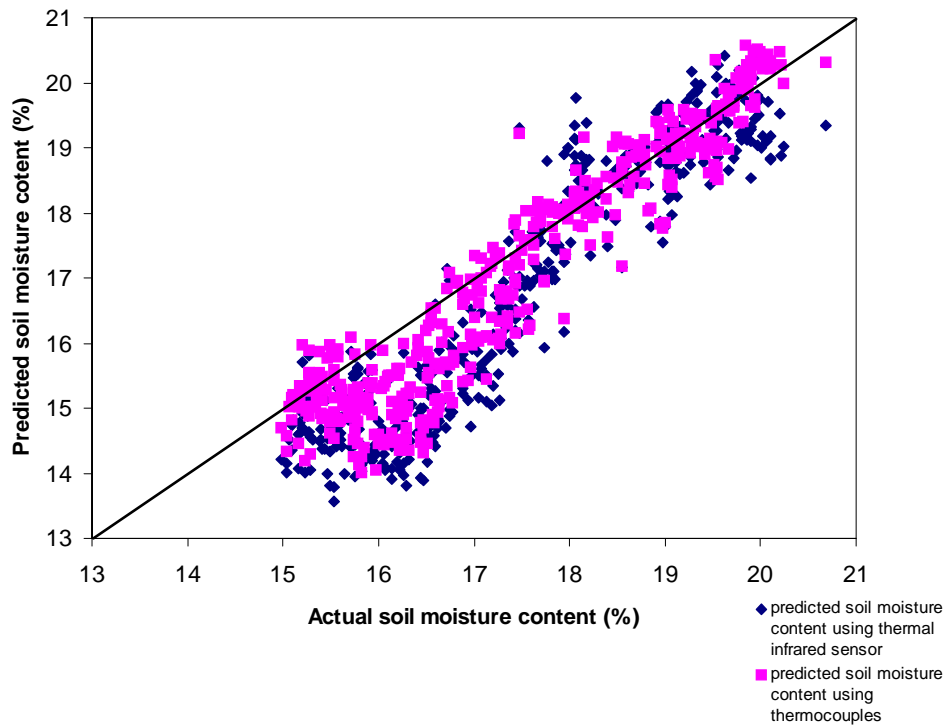
Figure 5.12 Actual versus predicted SMC measurements using thermocouple and the infrared sensor for MLR3 of sand non-compacted soil.

6. SUMMARY AND CONCLUSIONS

Measurements of soil moisture content (SMC), soil surface temperature (T_s), and metrological weather variables T_a, RH, SR, and WS were collected for a period of a day for 12 samples of two types of soils (clay/sand), and with two compaction levels (compacted/non-compacted). The soil moisture content ranged from a maximum of 20% at the beginning of the experiment to a minimum of 9.3% at the end. Furthermore, models to predict the SMC for each soil type and configuration were generated using stepwise multiple linear regression data analysis. In data analysis, the dependent variable was SMC and the independent variables were soil surface temperature-minus-ambient air temperature (T_d), relative humidity (RH), solar radiation (SR), and wind speed (WS). In general, the models showed good prediction performance. Models of larger size for all soil types and configuration showed better prediction performance than smaller models.

Models of different sizes for the same soil type and configuration were similar and had consistent coefficients. Models of clay soils with different configuration had higher T_d coefficients than those of sandy soil. Conversely, models of sandy soils had higher coefficients of RH than of clay soils. This indicates that differential temperature (T_d) had higher effect on clay soils than in sandy soils while relative humidity (RH) posed higher effect on sandy soils than in clay soils.

The best model for each soil type and configuration was determined by comparing the calibration R^2 and RMSE values along with validation RMSE values for models of different size. The best model for compacted clay soil was the three-variable model containing Td, RH, and SR with a calibration R^2 of 0.72, a calibration RMSE of 1.64, and a validation RMSE of 1.59. Model 3 is the best predictive model, favoring a reduction in size of the model to the smaller contribution of larger model (MLR4) in minimizing the RMSE value. Furthermore, the difference between RMSEC and the RMSEV values is only 0.05, which indicates that there is no significant over fitting toward the calibration data and that the model performs well for the entire range of the data. The best model for non-compacted clay soil was the three-variable model containing Td, RH, and SR, with a calibration R^2 of 0.72, a calibration RMSE of 1.14, and validation RMSE of 1.04. Similarly, this model was selected because it provided higher predictive performance than the smaller size models (MLR1 and MLR2) and comparable predictive performance like MLR4, while having fewer variables. The best model for compacted sandy soil was the two-variable model containing T_d and RH with a calibration R^2 of 0.86, a calibration RMSE of 0.99, and a validation RMSE of 1.00. This model had the highest calibration R^2 value (0.86) equal to those of MLR3 and MLR4 and the highest validation R^2 (0.86). It also had the lowest RMSEC value of (0.99) and validation RMSEV value of (1.00). This model combined two advantages: the small size (few variables) and higher prediction performance than the other models. The best model for non-compacted sandy soil was the three-variable model because with its fewer variables, it performed better than the larger model (MLR4) and also better than the smaller models (MLR1 and MLR2). This model contained T_d, RH and SR with a calibration R^2 of 0.82, a calibration RMSE of 1.05, and a validation RMSE of 1.07.

To be able to remotely measure the soil moisture content, a thermal infrared sensor was calibrated against the thermocouples that were used to measure soil surface temperature during the experiment. The collected measurements in this study were: the soil surface temperature measured by the thermal infrared sensor (T_{ir}), soil surface temperature as measured by the thermocouples (T_s), and sensor body temperature (T_{sens}) for three replications of soil samples: clay compacted soil, sand compacted soil, and sand non-compacted soil. A calibration model was generated to determine the corrected value of (T_{ir}), which was then used to calculate the soil surface-minus-air temperature (T_d) value. The calculated soil surface-minus-air temperature (T_d) value, using (T_{ir}), was used along with the measured meteorological variables (RH, SR, and WS) to estimate soil moisture content for the best selected models of sand compacted soil and sand non-compacted soil. Graphs were developed to compare between the predicted soil moisture content values using thermocouples and the predicted soil moisture content values using the thermal infrared sensor versus the actual soil moisture content values using the best selected models for compacted and non-compacted sandy soils. The thermal infrared sensor provided comparable predictive performance, relative to thermocouples.

7. RECOMMENDATIONS

The measurement of soil moisture content (SMC) using a non-contact method with a thermal infrared sensor and weather meteorological variables is very promising. This technique provides non-destructive, low-cost, and fast SMC measurement. In this study, the experiment was carried out on soil samples in containers. However, it is recommended to run the experiment in a field to ensure that the generated models will be more realistic and naturally representative of the correlation between SMC and the measured variables. In this study, linear regression models were generated in order to predict SMC from two soil types and two compaction levels. In future, the use of non-linear regression models for the prediction of SMC and for practical sensor development should be considered, which might improve the prediction performance. For the application of this technique for a specific field with known boundaries, it is recommended that the generated calibration models incorporate all the variations in the field regarding soil types, ranges of moisture content, and weather conditions. This will ensure that the produced models are more representative of the site whose SMC is to be remotely measured. Also, it is advisable to investigate the effect of vegetation cover on the sensor measurements and the generated predictive calibration models. The sensor used in this study was significantly affected by ambient temperature, which led to improper functioning of the sensor, which could lead to permanent failure of the sensor in the long term. Thus, it is advisable to use a sensor that is more resistive to ambient temperature and humidity.

REFERENCES

Batlivala, P.P. and F.T. Ulaby, 1976. Remotely sensing soil moisture with radar. RSL technical report 264-8. University of Kansas Center for Research , Inc., Lawrence, Kansas, August.

Blad, B.L., B.R. Gardner, D.G. Watts and N.G. Rosenburg. 1978. Remote sensing of crop water status. Nebraska Agricultural Experiment Station Journal series No.6546.Omaha,NE.

Carry, J.W. and S.A. Taylor. 1967. The dynamics of soil water. Part II. Temperature and solute effects. Agron. 11:245-253.

Chilar, J. 1976. Soil Moisture Determination by Thermal Infrared Remote Sensing: Paper presented at the Workshop of Remote sensing Of Soil Moisture and Ground Water, Toronto. Ontario, pp. 206-215.

Collet, L.S. 1976. Advances in Surface Geophysical Techniques for Groundwater and Soil Moisture: Paper presented at the Workshop of Remote sensing of Soil Moisture and Ground Water, Toronto. Ontario, pp. 51-62.

Dagnew, M.D. 2002. Reflectance spectroscopy sensing of hog manure nutrients. Msc Thesis, Univ. of Saskatchewan.

Davis, J.L., G.C. Topp, and A.P. Annan. 1976. Elecromagnetic detection of soil water content: Progress report II: Paper presented at the Workshop of Remote sensing of Soil Moisture and Ground Water, Toronto. Ontario, pp. 96-109.

De Griend, A. and M. Owe. 1994. Microwave vegetation optical depth and inverse modeling of soil emissivity using Nimbus/SMMR satellite observations,. *J. of Met. & Atm. Physics*, 54: 225-239.

De Jong, E.. 1976. Agriculture and soil moisture: Paper presented at the Workshop of Remote sensing Of Soil Moisture and Ground Water, Toronto. Ontario, pp. 3-9.

Duckworth, J. 1998. Spectroscopic quantitative analysis. In *Applied Spectroscopy: A Compact Reference for Practitioners*, eds. J. Workman, Jr. and A. Springsteen, 93-163. San Diego, CA: Academic Press.

Ehrler, W.L, S.B.Idso and R.J.Reginato. 1978. Diurnal changes in plant potential and canopy temperature of wheat as affected by drought. *Agronomy journal*.70:999-1004.

Gates, D. M. 1970. Physical and Physiological Properties of Plants .*Remote Sensing*, pp. 225-252.

Gillespie, A.R. and A.B.Kahle. 1977. Construction and interpretation of a digital thermal inertia image. *Photogrammetric Engineering and Remote Sensing* 43(8): 983-1007.

Heimovaara, T.J. and W.A. Bouten. 1990. Computer-controlled 36-channel time domain reflectometry system for monitoring soil water contents. *Water Resour. Res.* 26:2311–2316.

Holter, M.R., M. Moore, J.L. Beard, T.Limperis, and R.K. Moore. 1970. Imaging with nonphotographic sensors . *Remote Sensing* , pp. 73-161.

Idso, S.B. and W.L.Ehler. 1976. Estimating soil moisture in the root zone of crops: A technique adaptable to remote sensing. Geophysical Research Letters 3(1): 23-25.

Idso,S.B., R.D.Jackson, R.J.Reginato, B.A.Kimball, and F.S.Nakayama. 1975. The dependence of bare Soil Albedo on soil water content. *J.Appl. Meteorology*, 14, pp. 109-113.

Ingleby, H.R. 1999. Spectral reflectance measurements for organic matter sensing in Saskatchewan soils. M.Sc. thesis, Univ. of Saskatchewan.

Jackson, T. and P. O'Neill. 1990. Attenuation of soil microwave emission by corn and soybeans at 1.4 and 5 GHz,. *IEEE Trans. on Geos. & Rem. Sens.*, vol. 28(5), pp. 978-980.

Jackson, T., D. Le Vine, A. Hsu, A. Oldark, P. Starks, C. Swift, J. Isham, and M. Hakem. 1999. Soil moisture mapping at regional scales using microwave radiometry: the Southern Great Plains hydrology experiment,. *IEEE Trans. on Geos. & Rem. Sens.*, 37: 2136-2151.

Levitt, D.G. 1989. The use of reflected middle infrared and emmited thermal radiation in the remote sensing of soil water content. Msc Thesis, Univ. of Arizona.

Liew, S.C. 2006. Electromagnetic Waves (English). Centre for Remote Imaging, Sensing and Processing, National University of Singapore.

Luney, P.R. and H.W. Dill. 1970. Uses, Potentialities, and needs in agriculture and forestry .*Remote Sensing*, pp. 1-34.

Mahrer, Y. and R.A. Pielke. 1977. A numerical study of the airflow over irregular terrain. *Atmospheric Physics* 50: 98–113.

McCumber, M.C. and R.A. Pielke. 1981. Simulation of the effects of surface fluxes of heat and moisture in a mes. numerical model 1. *Journal of Geophysical Research* 86: 9929-9938.

Microsoft Corporation, 2002. Microsoft windows XP, home edition. Manual book.

Myers, V. I. 1967. Spectral sensing in agriculture. Ann. Rep. on NASA Contract R-09-038-002.Fruit, Vegetable, Soil and Water Research Laboratory, Agr. Res. Service, Dep. Agr., Washington, D. C., pp. 61-65.

Myhre, B.E., and S.F. Shih, 1990. Using Infrared Thermometry to Estimate Soil Water Content for a Sandy Soil. ASAE PAPER, Vol. 33(5): pp 1479-1486.

Myhre,B.E. 1988.Using thermal infared thermometry to estimate soil water content.M.E. thesis, Department of Agricultural Engineering , University of Florida, Gainsville.

Njoku, E., T. Koike, T. Jackson, and S. Paloscia, 2000, .Retrieval of soil moisture from AMSR data,. In *Microwave Radiometry and Remote Sensing of the Earth's Surface and Atmosphere*, P. Pampaloni and S. Paloscia (eds.), VSP, Utrecht, The Netherlands, pp. 525-533.

O'Neill, P., N. Chauhan,and T. Jackson. 1996. Use of active and passive microwave remote sensing for soil moisture estimation through corn,. *Int. J. of Rem. Sens*., 17: 1851-1865.

Russell, M.B. and L.W. Hurlbut. 1959. The agricultural water supply. *Adv. Agron*. 11:6-19.

SAS. 1999. SAS/STAT user's guide in: SAS online Doc®, version 8. Cary, NC: SAS Institute Inc.

Scherer, T. F. 1986. Canopy-air temperature differences as affected by soil textural class and growing season. Ph.D Thesis, Univ. of Minnesota.

Schmugge,T., P. Gloerson, T. Wilheit, and F. Geiger. 1974. Remote sensing of soil moisture with microwave radiometrs. *J.Geophys. Res*., 79, pp.317-323.

Shih,S.F., D.S.Harrison, A.G.Smajstrla and F.S.Zazueta. 1986. Using infrared thermometry data in soil moisture estimation.ASAE Paper No.86-2112.St. Joseph,MI:ASAE.

Taylor, S.A. 1966. Water retention characteristics of soils. In Environmental Biology, P.L. Altman and D.S. Dittmer (eds.). Federation of American Societies for Experimental Biology.

Taylor, S.A., D.D. Evans and W.D. Kemper. 1961. Evaluating soil water. Bulletin. 426, Agric. Exp. Station, Utah State University.

U.S. Soil Conservation Service. 1966. Aerial photo interpretation in classifying and mapping soils. Agr. Handbook No. 294. Dep. Agr., Washington, D. C., pp. 1-20.

Ulaby, F., R. Moore, and A. Fung. 1982. *Microwave Remote Sensing: Active and Passive, Vol. II*, Reading, MA, Addison-Wesley Publishing Co.

Ulaby, F.T . and P.P. Batlivala. 1976. Optimum radar parameters for mapping soil moisture. *IEEE Trans. On Geoscience Electronics*, vol. GE-14, no. 2, pp. 81-93, April.

Ulaby, F.T. 1975. Radar Response to vegetation. *IEEE Trans. On Antennas and propagation*, January, vol. Ap-23, no. 1, pp.36-45.

Ulaby, F.T. 1976. Evaluation of Radar as a Soil Moisture Sensor. workshop proceedings on remote sensing of soil moisture and ground water, Toronto. Ontario, Nov.8-10, pp. 169-183.

Ulaby,F.T., J. Chilar and R. K. Moore. 1974. Active Microwave Measurement of Soil Water Content. *Rem. Sens. of Env*, vol. 3, pp. 185-203.

Vleck, J. and D. King. 1983. Detection of subsurface soil moisture by thermal sensing: Results of laboratory, close-range, and aerial studies. *Photogrammetric Engineering and Remote Sensing* 49(11): 1593-1597.

Whiting, J.M., G. 1976. Airborne thermal infrared sensing of soil moisture and groundwater: Paper presented at the Workshop of Remote sensing Of Soil Moisture and Ground Water, Toronto. Ontario, pp. 145-154.

Wigneron, J.P., A. Chanzy, J-C. Calvet, and N. Bruguier. 1995. A simple algorithm to retrieve soil moisture and vegetation biomass using microwave measurements over crop fields,. *Rem. Sens. of Env.*, 51: 331-341.

APPENDIX A: TABLES

Table A.1 OS 34 L infrared sensor specifications

Resolution	0.1°C or 0.1°F
Accuracy	: ±0.5°C or ±1.0°F
Repeatability	±1.0°C or ±1.0°F
Temperature Range	-40 to 100°C
Spectral response	8 to 14 microns
Output	–mV standard; optional 4 to 20 mA, 0 to 5V
Input Power	External 5 to 26 Vdc @ 10 mA; 15 to 26 Vdc for
Emmisivity	Preset at 0.98
Response Time	0.25 sec
Dimensions	51 dia x 78.5 mm L
Weight	0.45 Kg

APPENDIX B: FIGURES

1. Figures B1 – B2: Measurements of replications 1 and 3 of compacted clay soil

2. Figures B3 – B4: Measurements of replications 1 and 3 of not-compacted clay soil

3. Figures B5 – B6: Measurements of replications 1 and 3 of compacted sandy soil

4. Figures B7– B8: Measurements of replications 1 and 3 of not-compacted sandy soil

5. Figures B9– B10: Measurements of replications 1 and 3 for sensor calibration
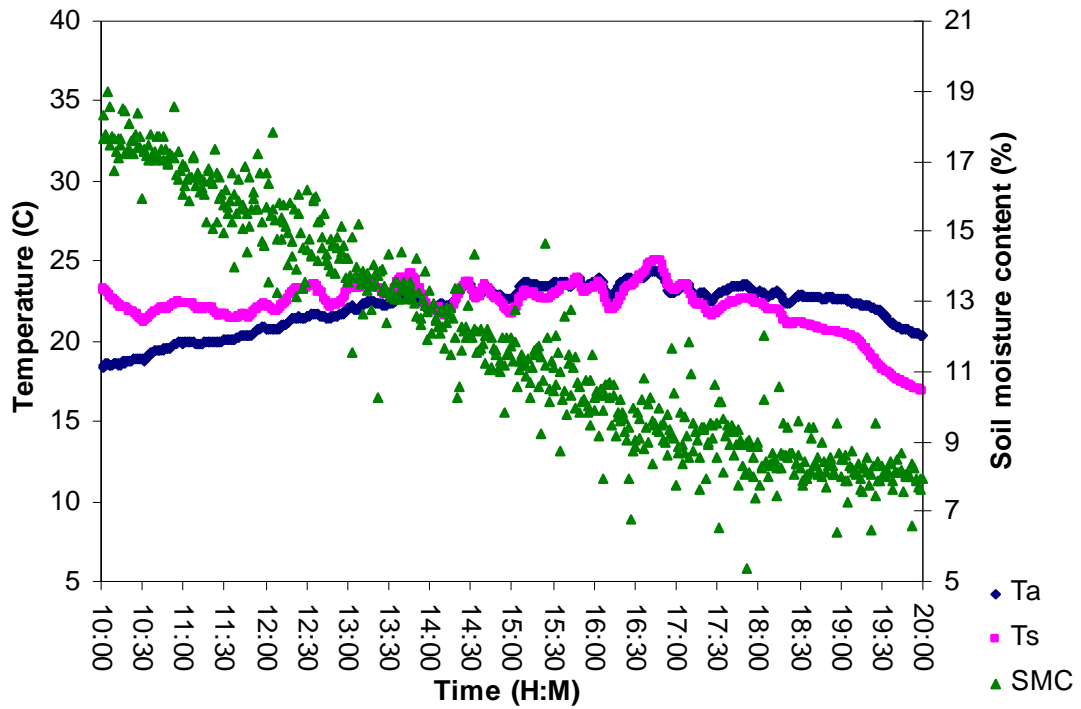
Figure B.1 Air temperature (T_a), soil surface temperature (T_s), and soil moisture content (SMC) versus time for replication 1 of compacted clay soil.
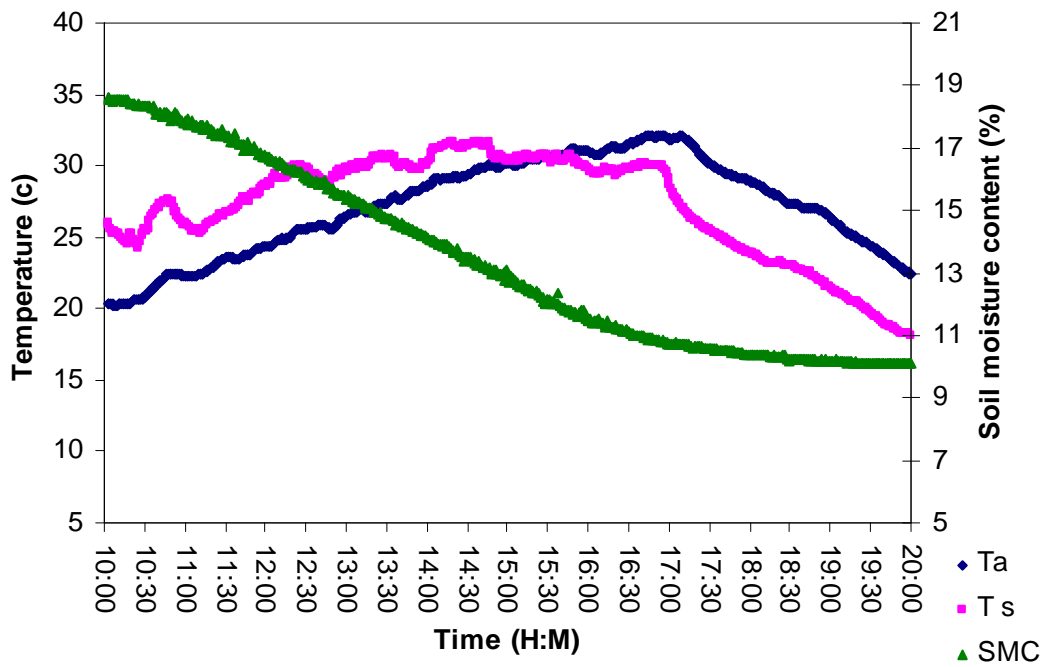
Figure B.2 Air temperature (T_a), soil surface temperature (T_s), and soil moisture content SMC versus time for replication 3 of compacted clay soil.
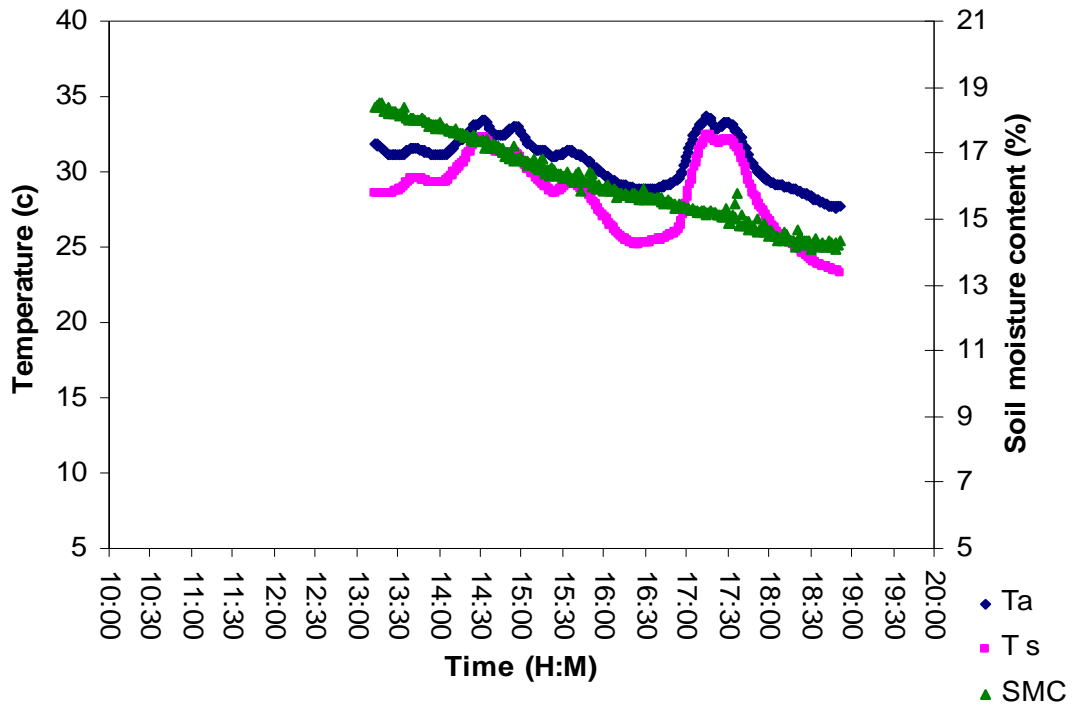
Figure B.3 Air temperature (Ta), soil surface temperature (Ts), and soil moisture content (SMC) versus time for replication 1 of non-compacted clay soil
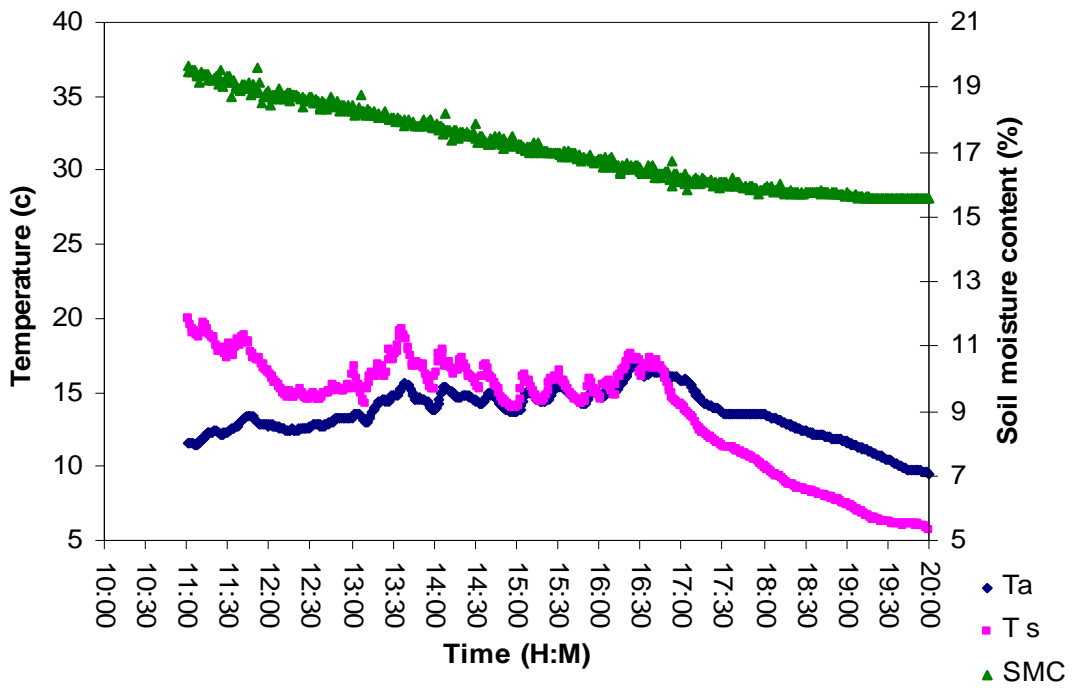
Figure B.4 Air temperature (T_a), soil surface temperature (T_s), and soil moisture content (SMC) versus time for replication 3 of non-compacted clay soil.
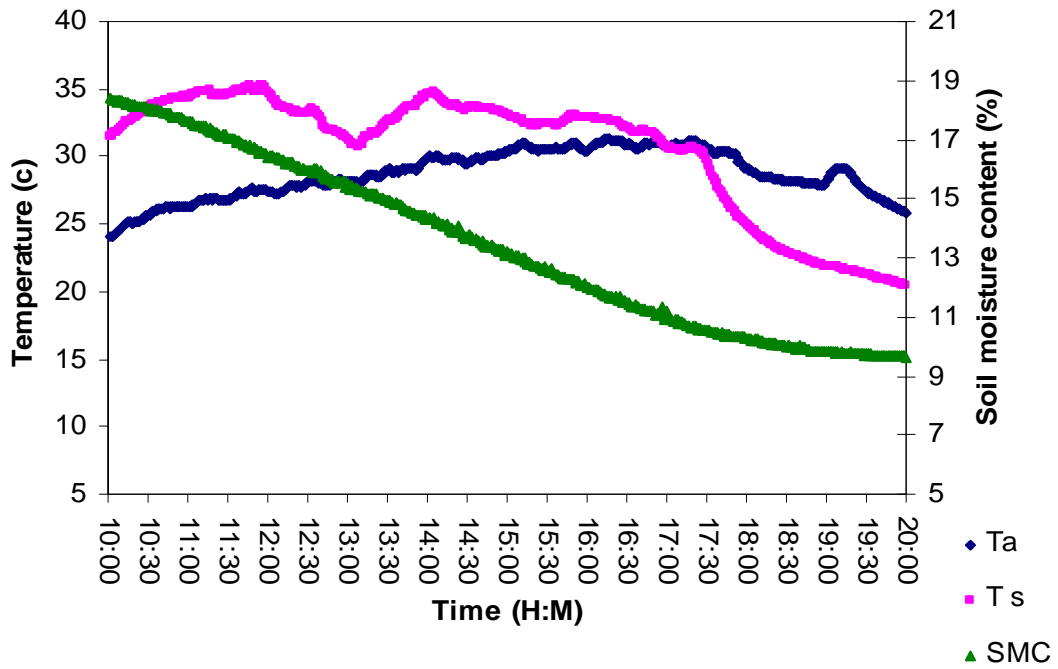
Figure B.5 Air temperature (T_a), soil surface temperature (T_s), and soil moisture content (SMC) versus time for replication 1 of compacted sandy soil.
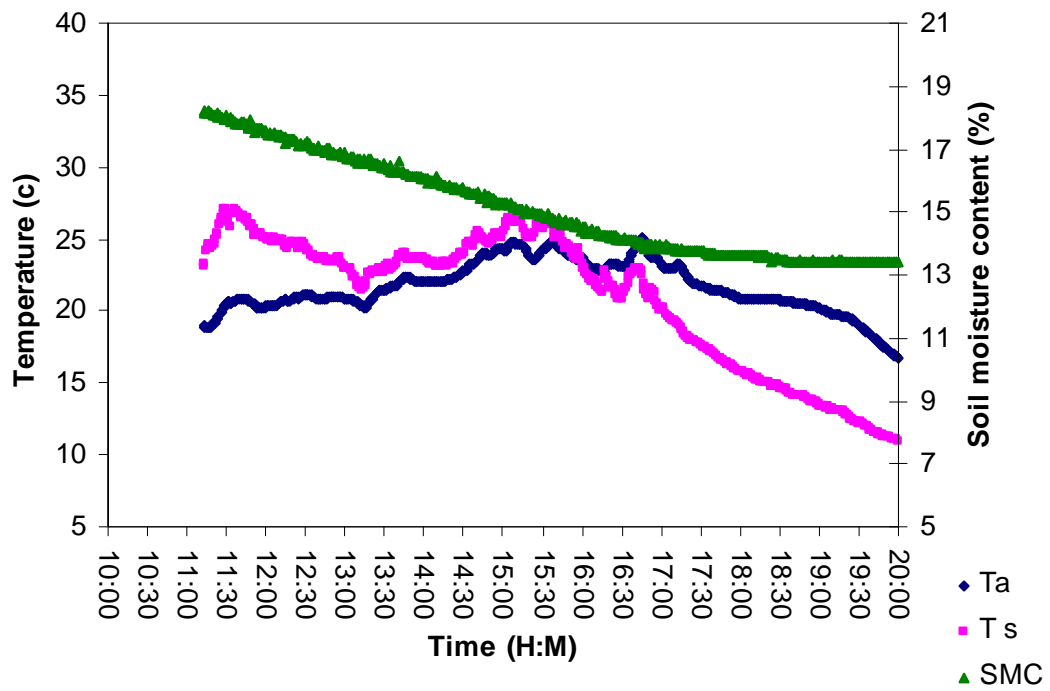
Figure B.6 Air temperature (T_a), soil surface temperature (T_s), and soil moisture content (SMC) versus time for replication 3 of compacted sandy soil.
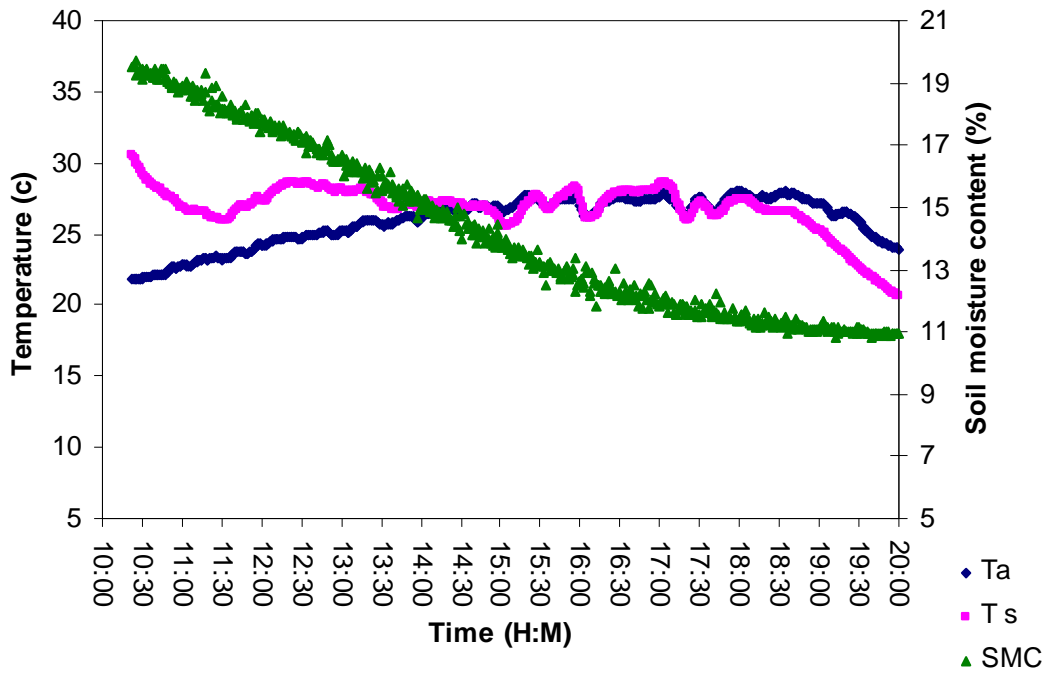
Figure B.7 Air temperature (T_a), soil surface temperature (T_s), and soil moisture content (SMC) versus time for replication 1 of non-compacted sandy soil.
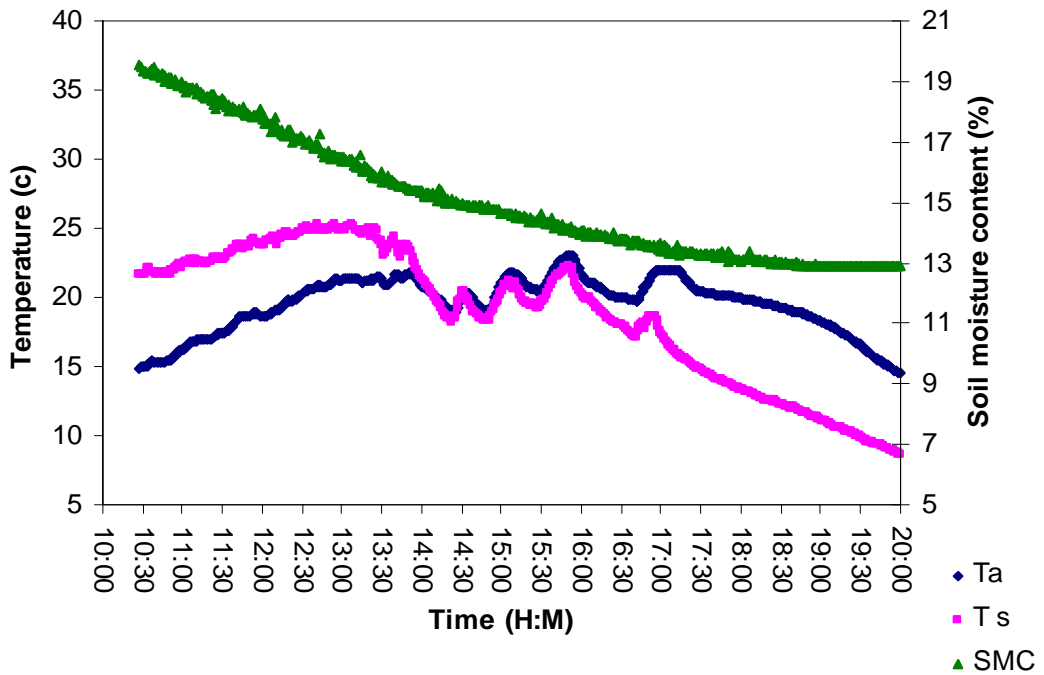
Figure B.8 Air temperature (T_a), soil surface temperature (T_s), and soil moisture content (SMC) versus time for replication 3 of non-compacted sandy soil
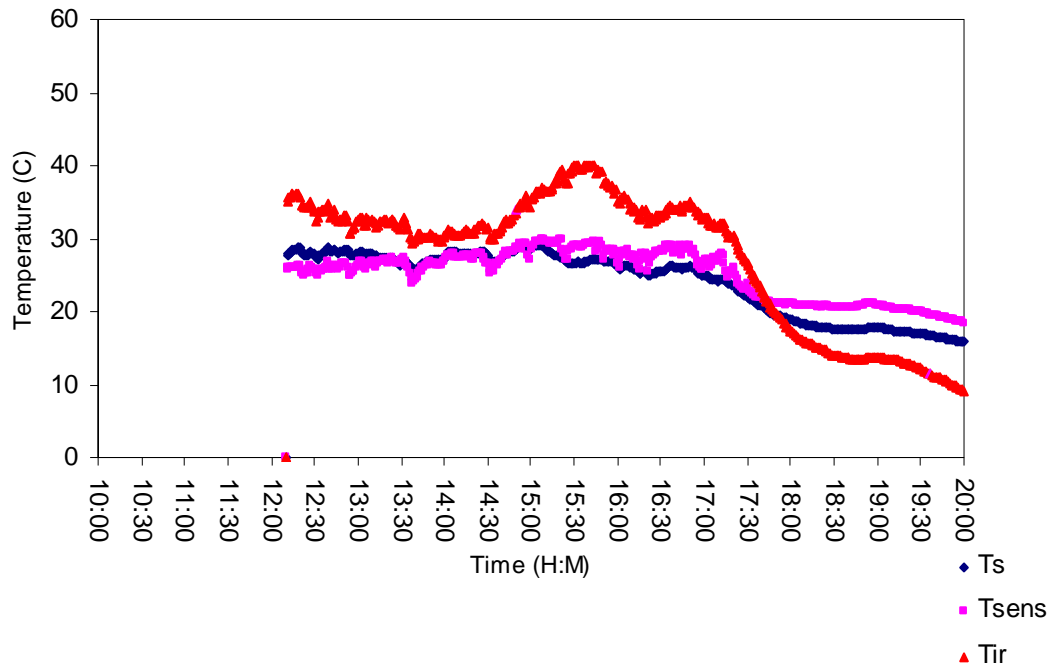
Figure B.9 Soil surface temperature measured by thermocouple (T_s), Soil surface temperature measured by the sensor (T_{ir}), sensor body temperature (T_{sens}) for second replication
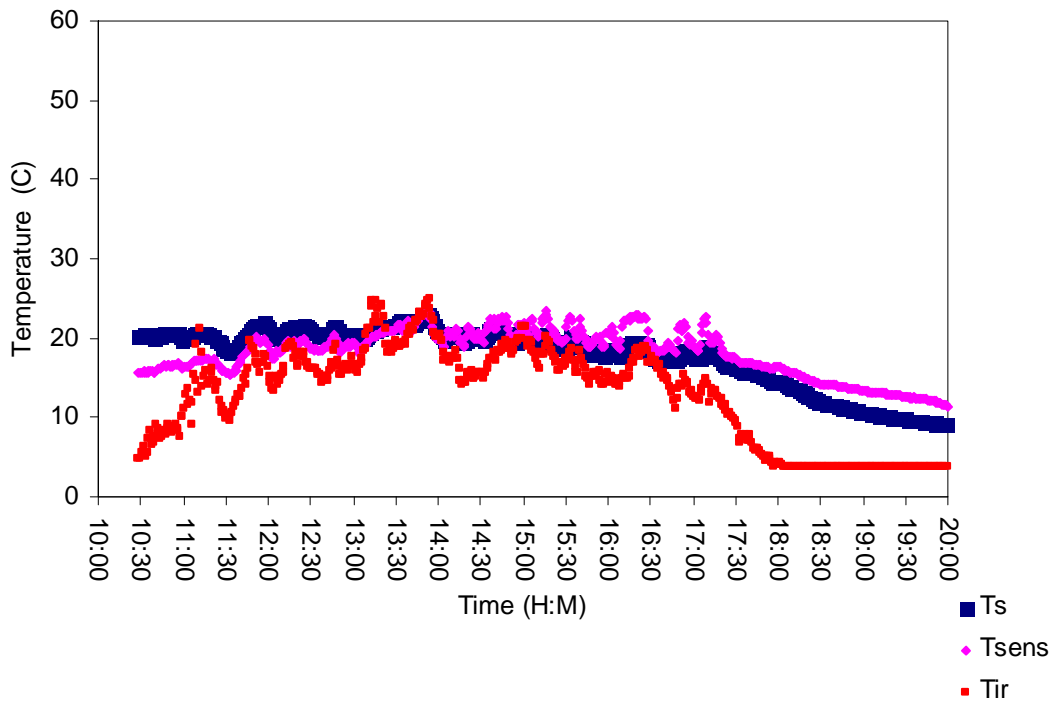
Figure 0.10 Soil surface temperature measured by thermocouple (T_s), Soil surface temperature measured by the sensor (T_{ir}), sensor body temperature (T_{sens}) for third replication

APPENDIX C: PREDICTED VERSUS ACTUAL SMC PLOTS

1. Figures C1 – C4: Compacted clay soil MLR models

2. Figures C5 – C8: Not- compacted clay soil MLR models

3. Figures C9 – C12: Compacted sandy soil MLR models

4. Figures C13– C16: Not- compacted sandy soil MLR models
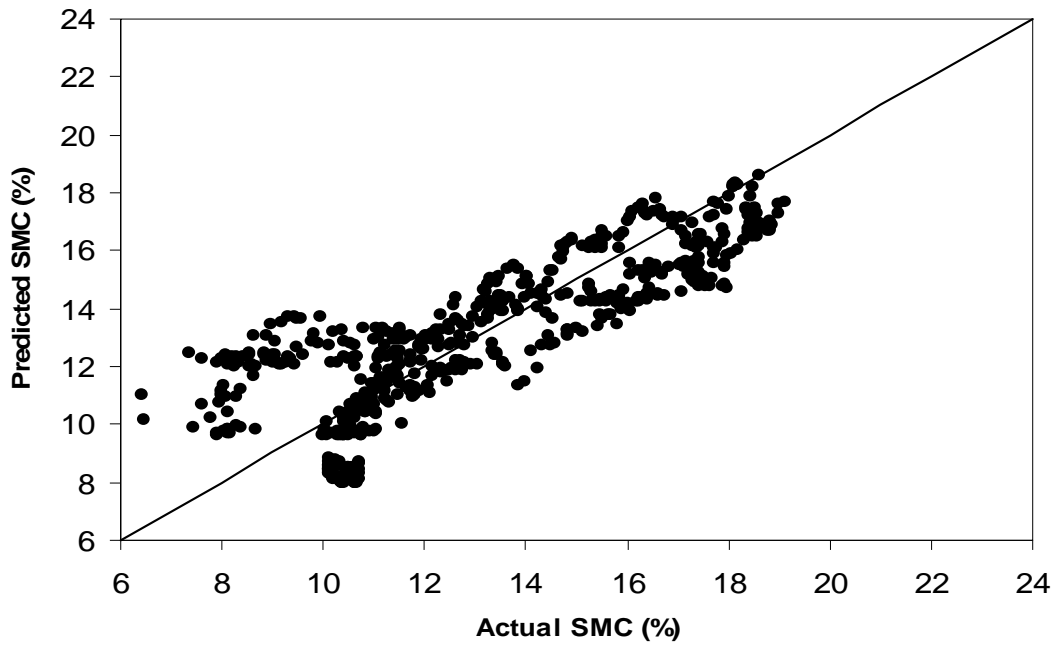
Figure C.1 Predicted versus actual soil moisture content (SMC) of compacted clay soil
for the one-variable model (MLR1)

The 1:1 line is Y = 1 * X, not the regression line
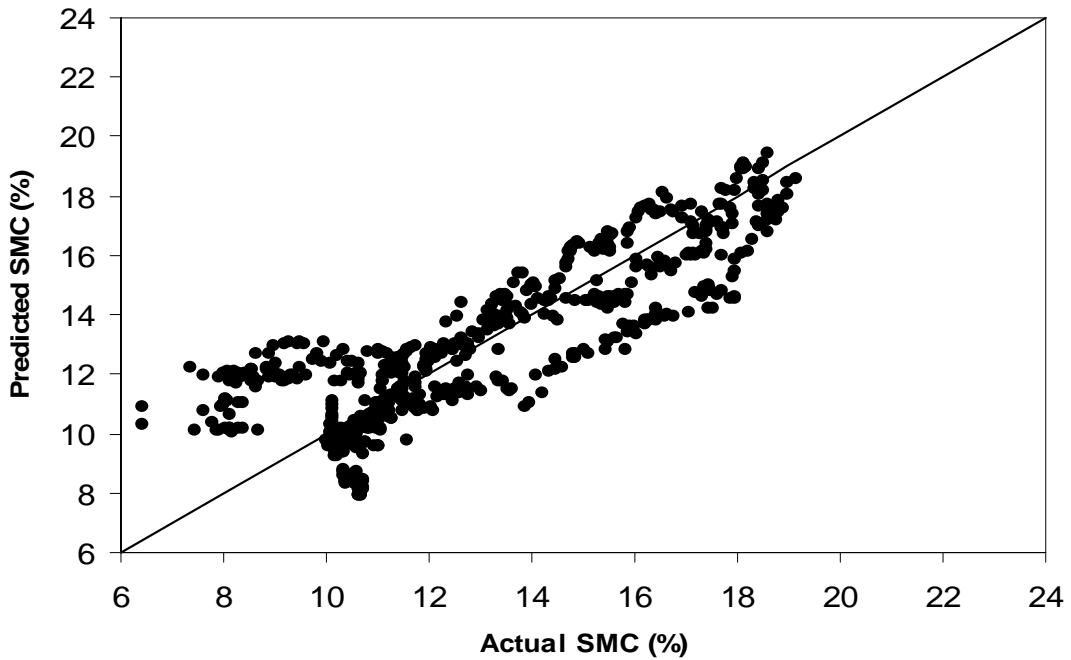
Figure C.2 Predicted versus actual soil moisture content (SMC) of compacted clay soil
for the two-variable model (MLR2)

The 1:1 line is Y = 1 * X, not the regression line
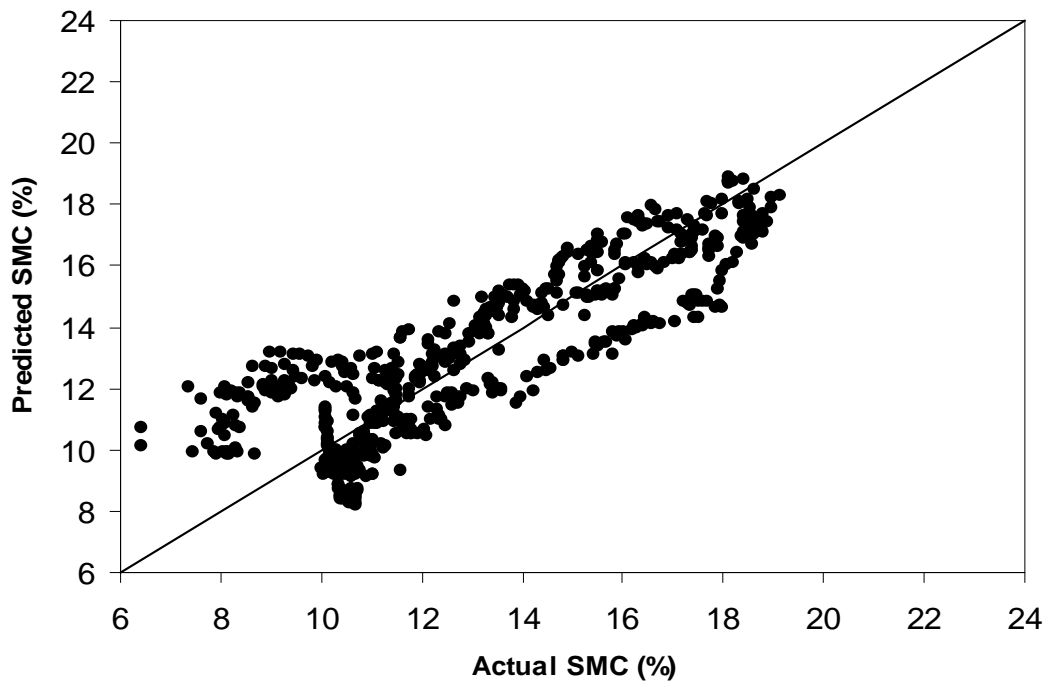
Figure C.3 Predicted versus actual soil moisture content (SMC) of compacted clay soil for the three-variable model (MLR3)

The 1:1 line is Y = 1 * X, not the regression line
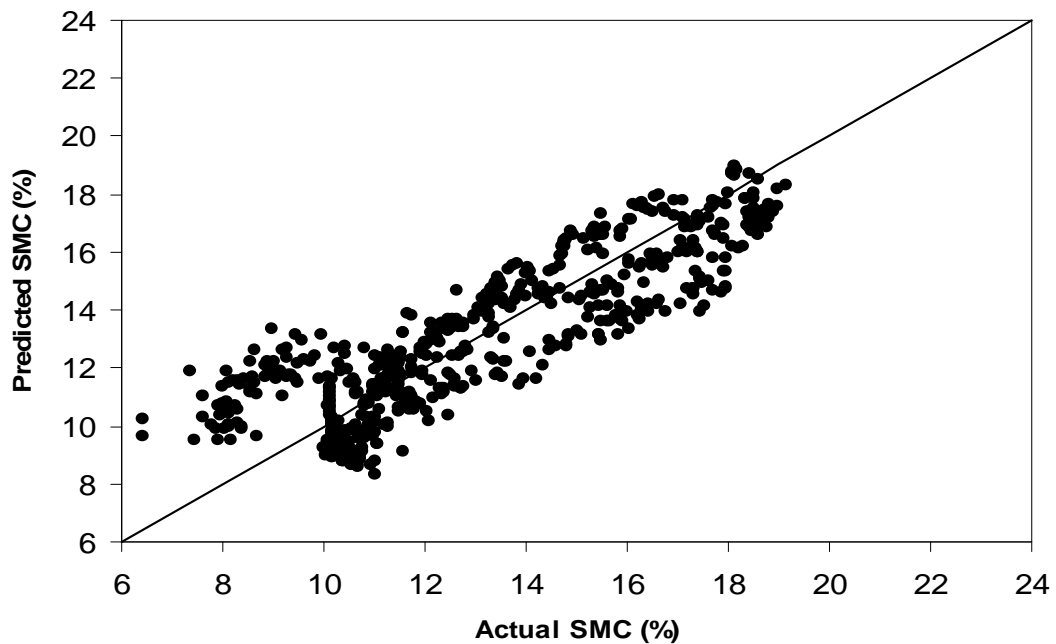
Figure C.4 Predicted versus actual soil moisture content (SMC) of compacted clay soil for the four-variable model (MLR4)

The 1:1 line is Y = 1 * X, not the regression line
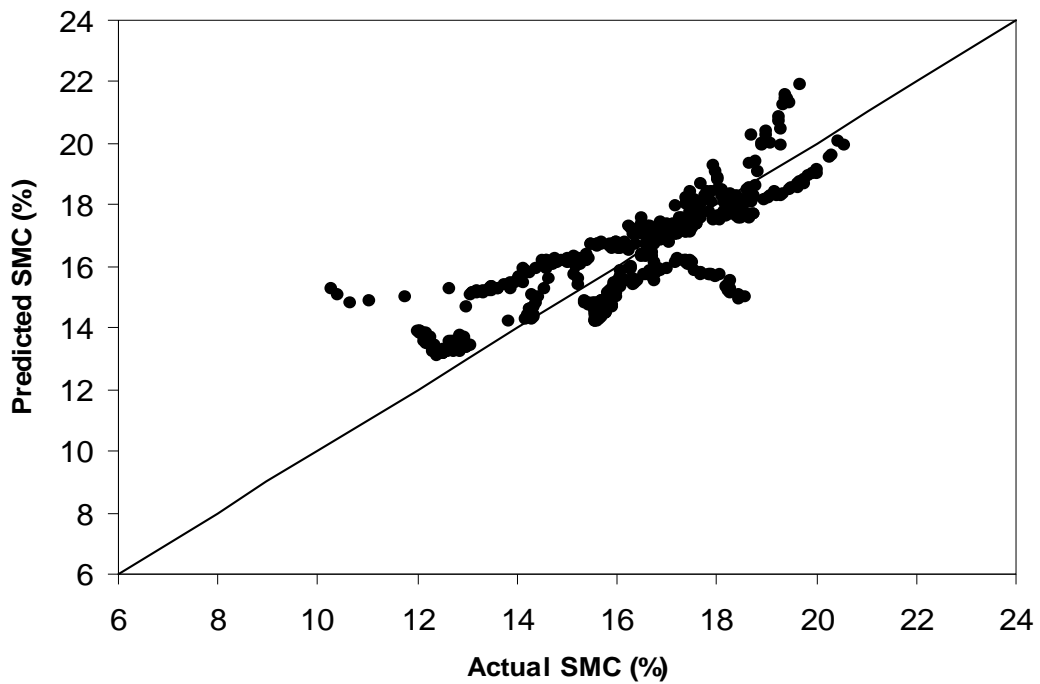
Figure C.5 Predicted versus actual soil moisture content (SMC) of non compacted clay soil for the one-variable model (MLR1)
The 1:1 line is Y = 1 * X, not the regression line
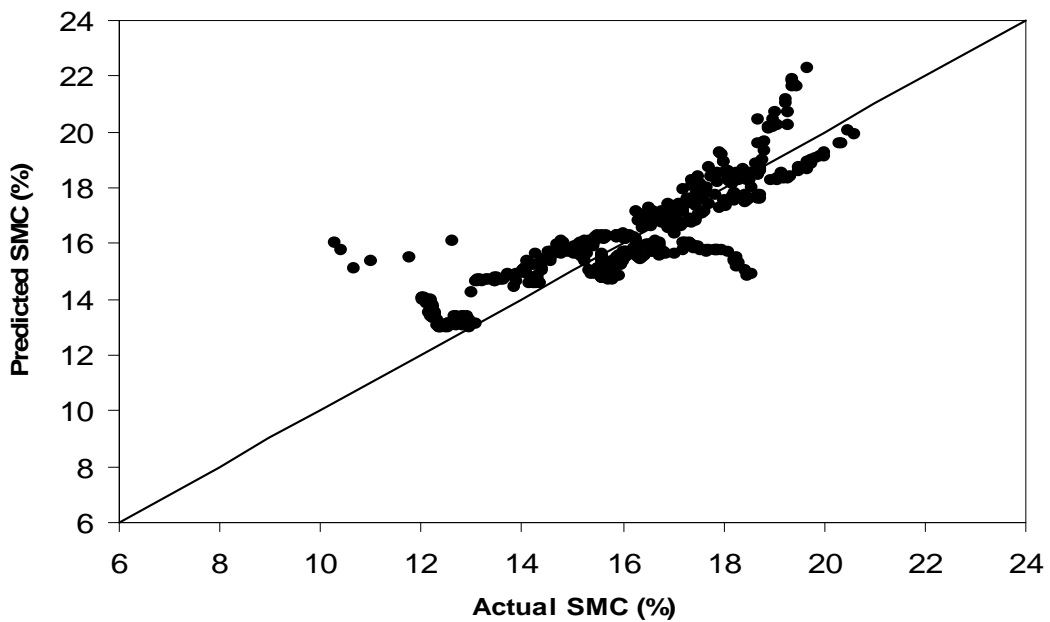
Figure C.6 Predicted versus actual soil moisture content (SMC) of non compacted clay soil for the two-variable model (MLR2)
The 1:1 line is Y = 1 * X, not the regression line
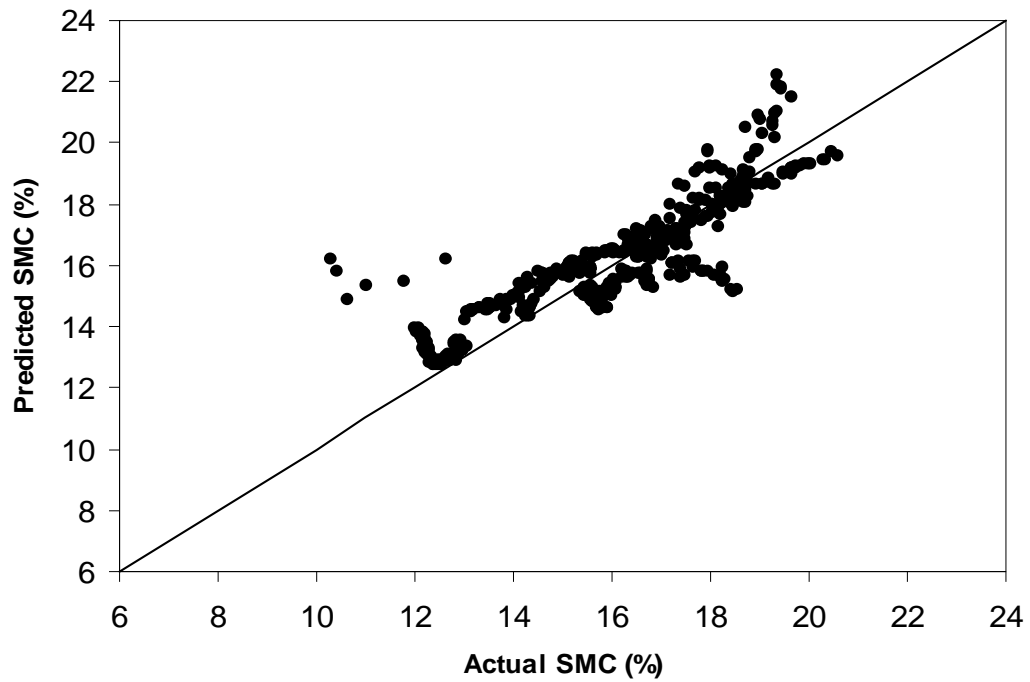
Figure C.7 Predicted versus actual soil moisture content (SMC) of non compacted clay soil for the three-variable model (MLR3)
The 1:1 line is Y = 1 * X, not the regression line
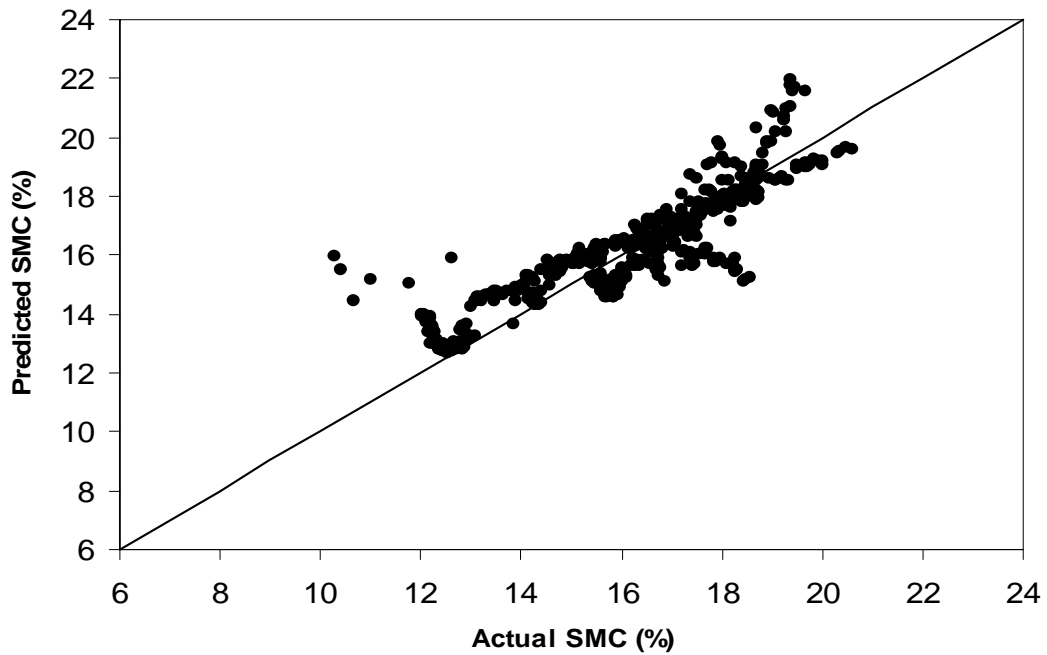
Figure C.8 Predicted versus actual soil moisture content (SMC) of non compacted clay soil for the four-variable model (MLR4)
The 1:1 line is Y = 1 * X, not the regression line
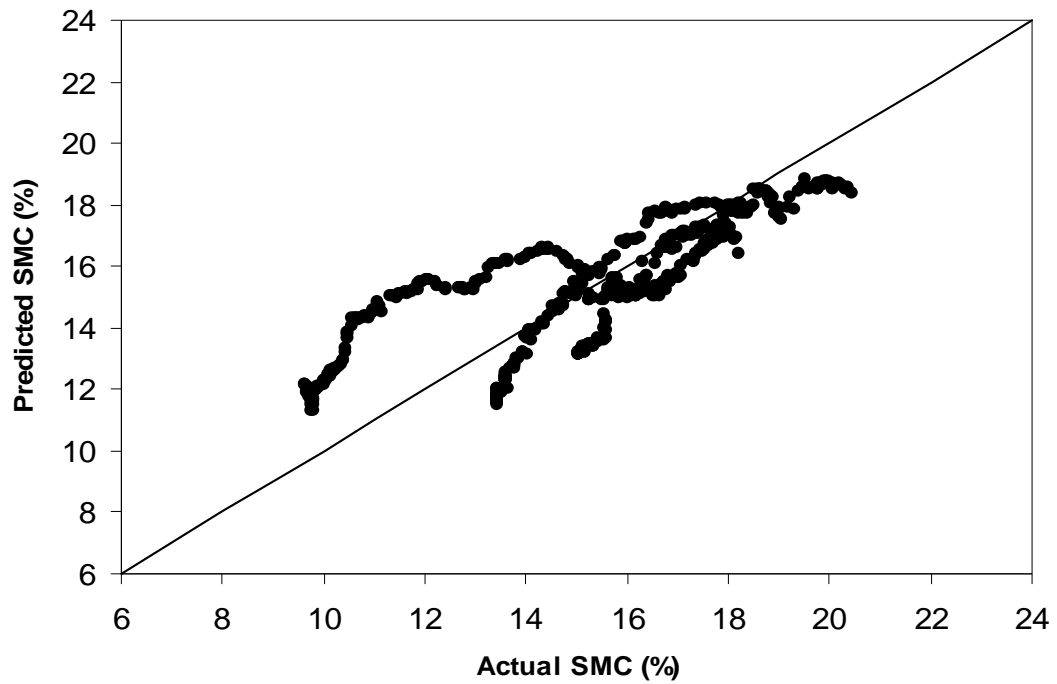
Figure C.9 Predicted versus actual soil moisture content (SMC) of compacted sandy soil for the one-variable model (MLR1)

The 1:1 line is Y = 1 * X, not the regression line
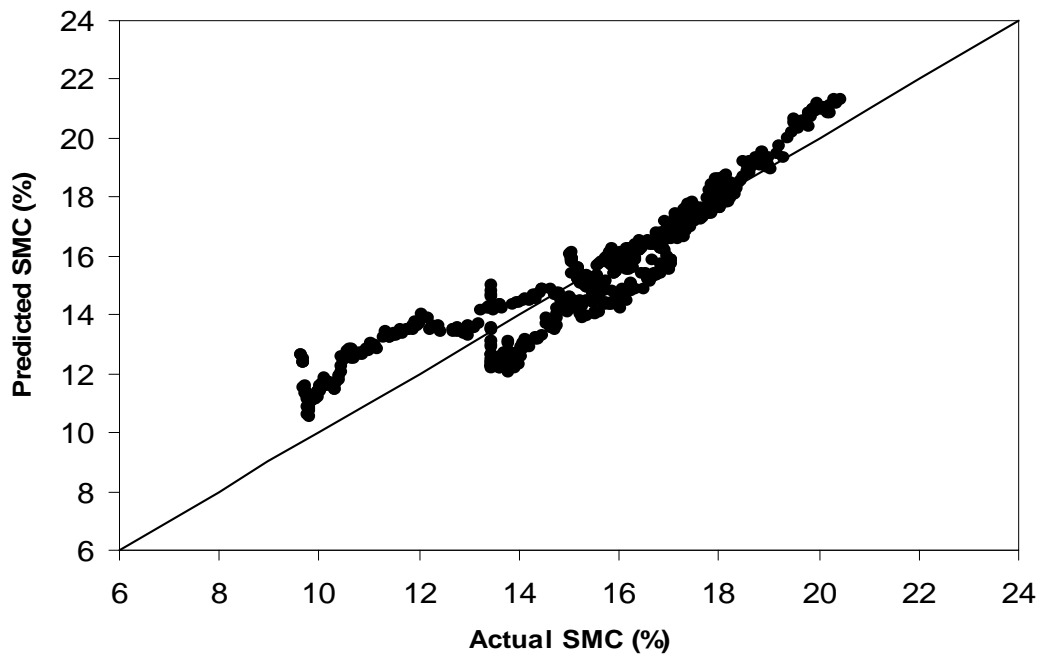
Figure C.10 Predicted versus actual soil moisture content (SMC) of compacted sandy soil for the two-variable model (MLR2)

The 1:1 line is Y = 1 * X, not the regression line
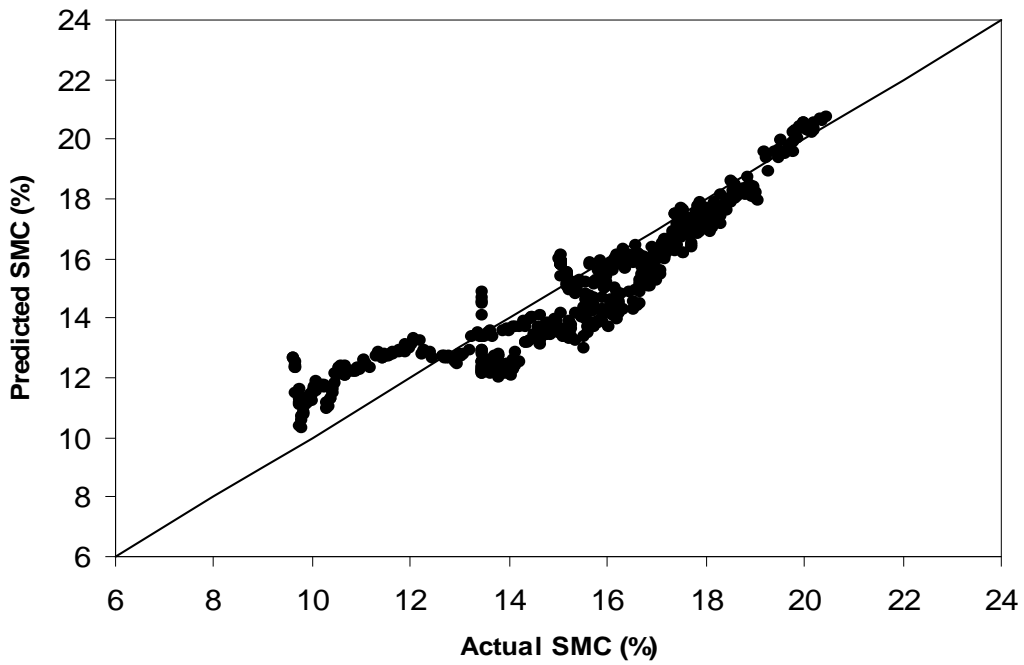
Figure C.11 Predicted versus actual soil moisture content (SMC) of compacted sandy soil for the three-variable model (MLR3)

The 1:1 line is Y = 1 * X, not the regression line
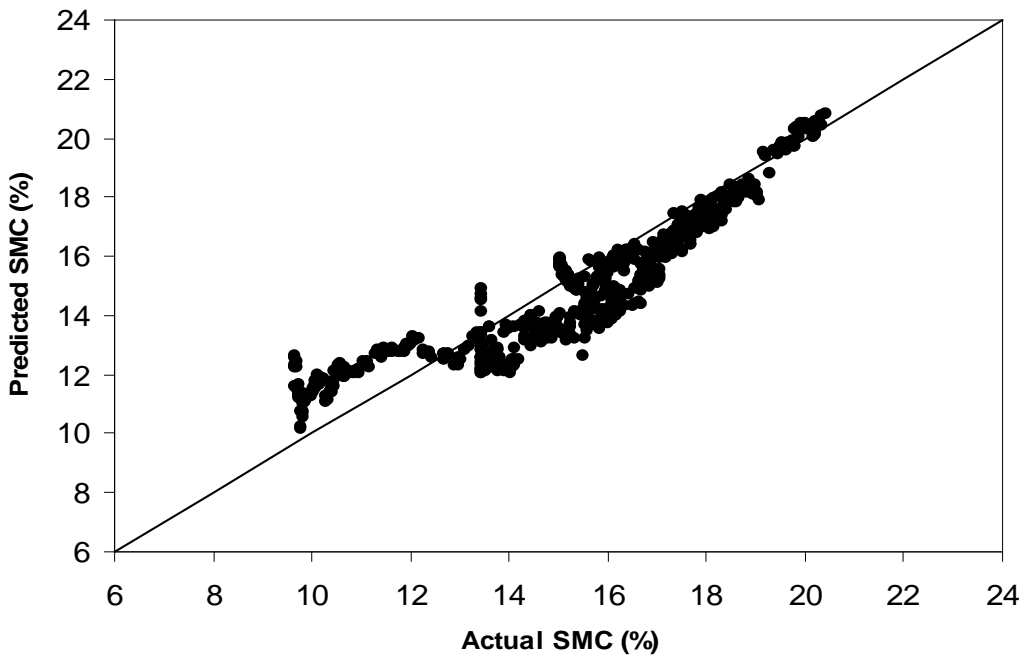
Figure C.12 Predicted versus actual soil moisture content (SMC) of compacted sandy soil for the four-variable model (MLR4)

The 1:1 line is Y = 1 * X, not the regression line
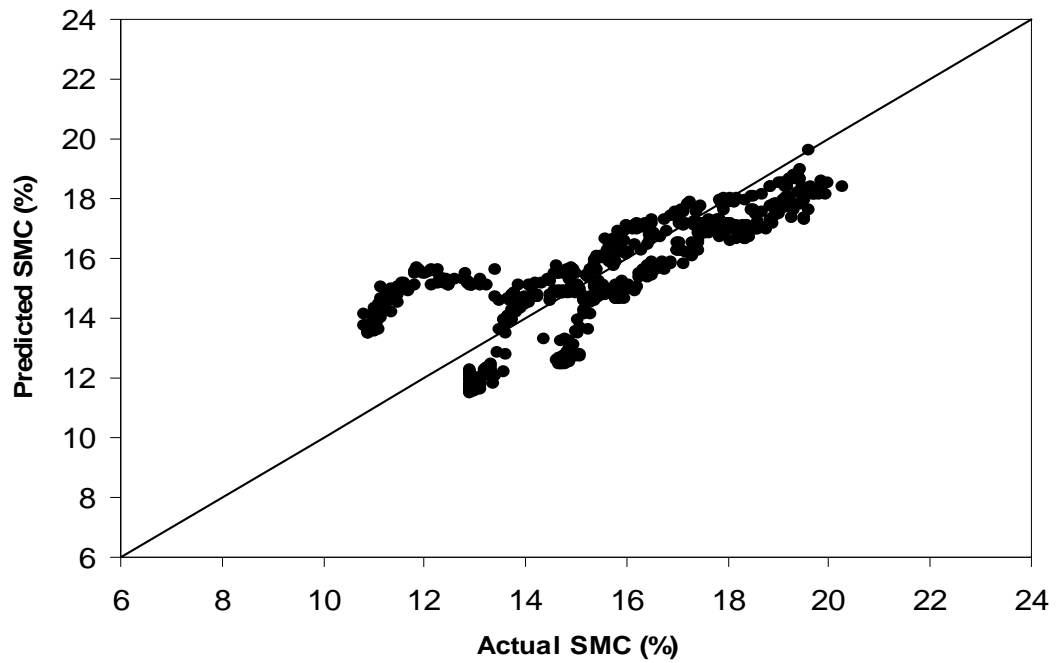
Figure C.13 Predicted versus actual soil moisture content (SMC) of non compacted
sandy soil for the one-variable model (MLR1)
The 1:1 line is Y = 1 * X, not the regression line
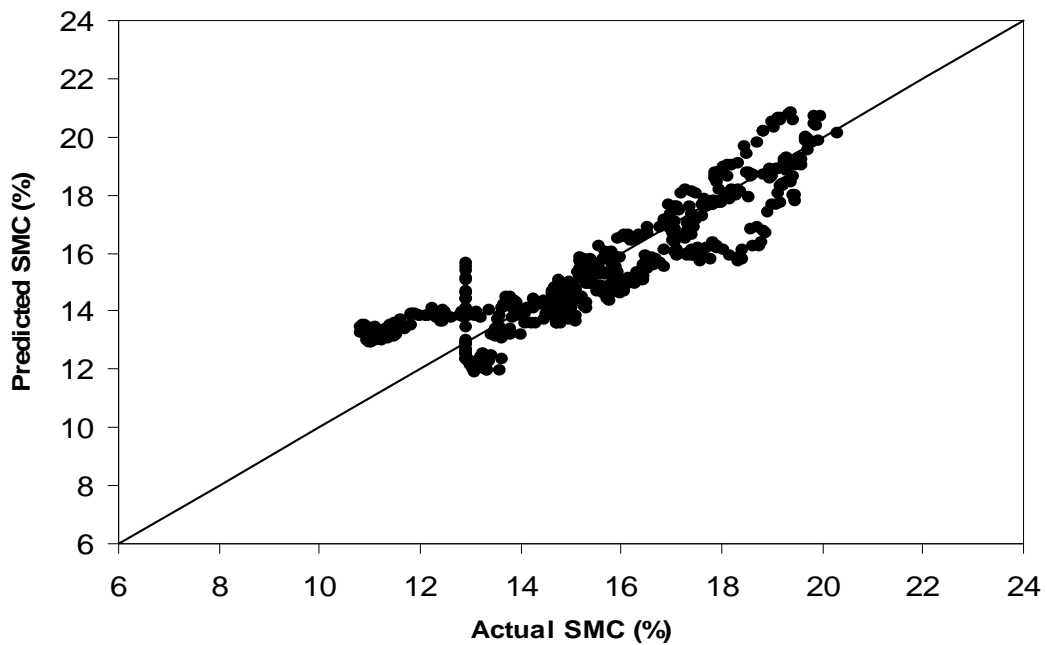
Figure C.14 Predicted versus actual soil moisture content (SMC) of non compacted
sandy soil for the two-variable model (MLR2)
The 1:1 line is Y = 1 * X, not the regression line
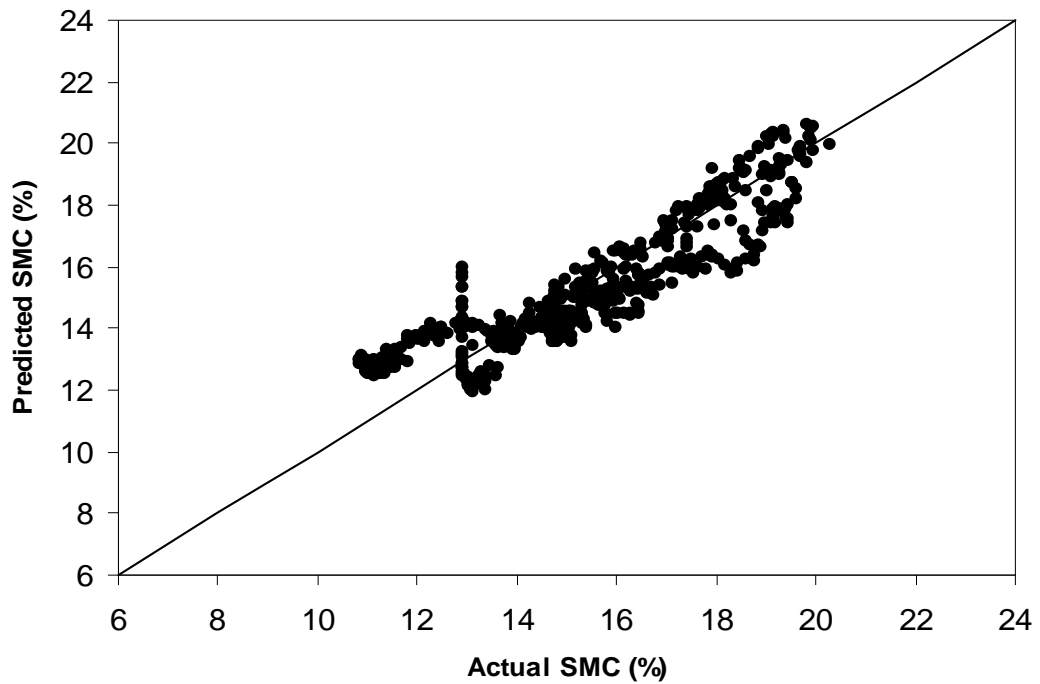
Figure C.15 Predicted versus actual soil moisture content (SMC) of non compacted sandy soil for the three-variable model (MLR3)
The 1:1 line is Y = 1 * X, not the regression line
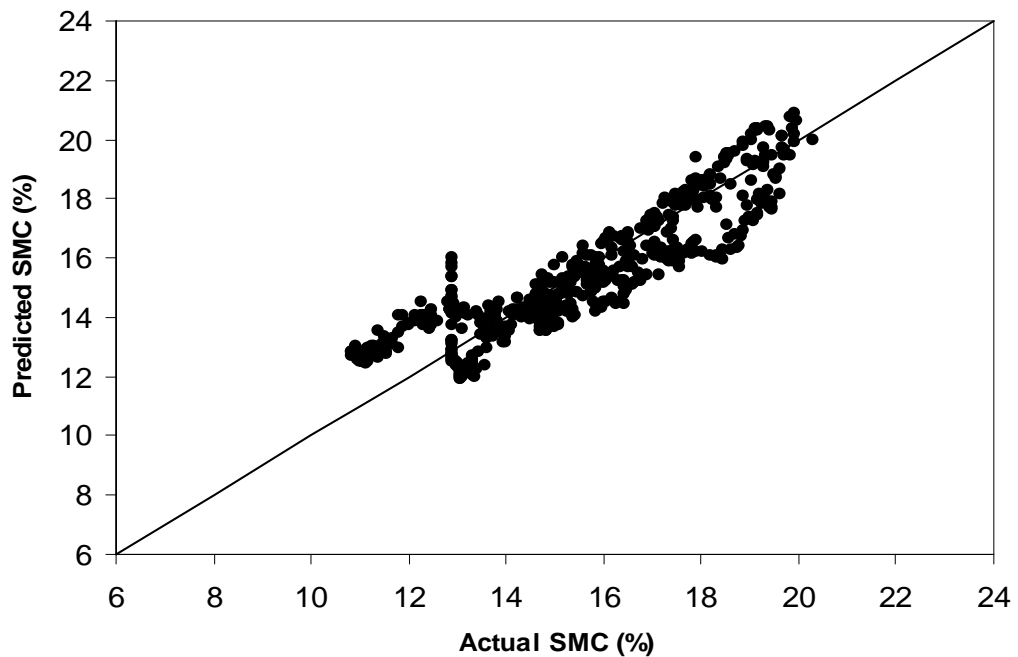
Figure C.16 Predicted versus actual soil moisture content (SMC) of non compacted sandy soil for the four-variable model (MLR4)
The 1:1 line is Y = 1 * X, not the regression line

APPENDIX D: SAS OUPUT (REGRESSION ANALYSIS)

1. Compacted clay soil

```
                         The REG Procedure
                           Model: MODEL1
                     Dependent Variable: __mc mc

                      Stepwise Selection: Step 1

        Variable Td Entered: R-Square = 0.6783 and C(p) = 234.6425


                        Analysis of Variance

                                   Sum of          Mean
        Source              DF     Squares        Square    F Value   Pr > F

        Model                1   7853.65870    7853.65870   2515.84   <.0001
        Error             1193   3724.17437       3.12169
        Corrected Total   1194      11578

                        Parameter     Standard
        Variable         Estimate        Error   Type II SS  F Value  Pr > F

        Intercept        13.06405      0.05117       203466  65178.1  <.0001
        Td                0.98993      0.01974   7853.65870  2515.84  <.0001

                   Bounds on condition number: 1, 1
------------------------------------------------------------------------------
                      Stepwise Selection: Step 2


        Variable _RH Entered: R-Square = 0.7099 and C(p) = 96.9405


                        Analysis of Variance

                                   Sum of          Mean
        Source              DF     Squares        Square    F Value   Pr > F

        Model                2   8218.59914    4109.29957   1458.16   <.0001
        Error             1192   3359.23394       2.81815
        Corrected Total   1194      11578

                        Parameter     Standard
        Variable         Estimate        Error   Type II SS  F Value  Pr > F

        Intercept        10.49897      0.23059   5842.02005  2073.00  <.0001
        Td                0.88010      0.02109   4907.73666  1741.48  <.0001
        _RH               0.06996      0.00615    364.94044   129.50  <.0001

               Bounds on condition number: 1.2649, 5.0595
------------------------------------------------------------------------------
                      Stepwise Selection: Step 3


                         The REG Procedure
                           Model: MODEL1
                     Dependent Variable: __mc  mc

                      Stepwise Selection: Step 3

        Variable SR Entered: R-Square = 0.7212 and C(p) = 48.6994


                        Analysis of Variance

                                   Sum of          Mean
        Source              DF     Squares        Square    F Value   Pr > F

        Model                3   8349.84279    2783.28093   1026.92   <.0001
```

```
Error                      1191    3227.99029        2.71032
Corrected Total            1194       11578


                        Parameter     Standard
            Variable    Estimate        Error    Type II SS  F Value  Pr > F

            Intercept    8.79521      0.33329    1887.37776   696.37  <.0001
            Td           0.70750      0.03230    1300.72897   479.92  <.0001
            SR        0.00095926   0.00013785     131.24365    48.42  <.0001
            _RH          0.09071      0.00673     492.95024   181.88  <.0001

              Bounds on condition number: 3.0841, 21.301
-----------------------------------------------------------------------------------
                       Stepwise Selection: Step 4


          Variable WS Entered: R-Square = 0.7315 and C(p) = 5.0000


                          Analysis of Variance

                                 Sum of          Mean
        Source           DF      Squares        Square     F Value   Pr > F

        Model             4    8469.22239    2117.30560     810.52   <.0001
        Error          1190    3108.61068       2.61228
        Corrected Total 1194       11578


                        Parameter     Standard
            Variable    Estimate        Error    Type II SS  F Value  Pr > F

            Intercept   10.07388      0.37795    1855.89088   710.45  <.0001
            Td           0.70362      0.03171    1286.09989   492.33  <.0001
            SR           0.00107   0.00013628     160.37593    61.39  <.0001
            _RH          0.07790      0.00687     335.91089   128.59  <.0001
            WS          -0.33540      0.04961     119.37961    45.70  <.0001

-----------------------------------------------------------------------------------
```

2. Not-compacted clay soil

```
                          The REG Procedure
                           Model: MODEL1
                      Dependent Variable: __mc  mc

                       Stepwise Selection: Step 1

          Variable Td Entered: R-Square = 0.6815 and C(p) = 150.7469


                          Analysis of Variance

                                 Sum of          Mean
        Source           DF      Squares        Square     F Value   Pr > F

        Model             1    3202.26575    3202.26575    2139.50   <.0001
        Error          1000    1496.73231       1.49673
        Corrected Total 1001    4698.99806


                        Parameter     Standard
            Variable    Estimate        Error    Type II SS  F Value  Pr > F

            Intercept   16.87467      0.04094        254240   169863  <.0001
            Td           0.60483      0.01308    3202.26575  2139.50  <.0001

              Bounds on condition number: 1, 1
-----------------------------------------------------------------------------------
```

Stepwise Selection: Step 2

Variable _RH Entered: R-Square = 0.7026 and C(p) = 76.4229

Analysis of Variance

Source	DF	Sum of Squares	Mean Square	F Value	Pr > F
Model	2	3301.71026	1650.85513	1180.29	<.0001
Error	999	1397.28781	1.39869		
Corrected Total	1001	4698.99806			

Variable	Parameter Estimate	Standard Error	Type II SS	F Value	Pr > F
Intercept	15.22591	0.19950	8146.95007	5824.71	<.0001
_RH	0.03473	0.00412	99.44451	71.10	<.0001
Td	0.57884	0.01301	2768.34988	1979.25	<.0001

Bounds on condition number: 1.0595, 4.2379

Stepwise Selection: Step 3

The REG Procedure
Model: MODEL1
Dependent Variable: __mc mc

Stepwise Selection: Step 3

Variable SR_ Entered: R-Square = 0.7215 and C(p) = 10.3743

Analysis of Variance

Source	DF	Sum of Squares	Mean Square	F Value	Pr > F
Model	3	3390.37258	1130.12419	861.87	<.0001
Error	998	1308.62548	1.31125		
Corrected Total	1001	4698.99806			

Variable	Parameter Estimate	Standard Error	Type II SS	F Value	Pr > F
Intercept	12.83586	0.34899	1773.82463	1352.78	<.0001
SR_	0.00099491	0.00012099	88.66232	67.62	<.0001
_RH	0.06706	0.00560	188.01907	143.39	<.0001
Td	0.44601	0.02049	621.58990	474.04	<.0001

Bounds on condition number: 3.1372, 24.084

Stepwise Selection: Step 4

Variable Ws Entered: R-Square = 0.7236 and C(p) = 5.0000

Analysis of Variance

Source	DF	Sum of Squares	Mean Square	F Value	Pr > F
Model	4	3399.98077	849.99519	652.37	<.0001
Error	997	1299.01729	1.30293		
Corrected Total	1001	4698.99806			

Variable	Parameter Estimate	Standard Error	Type II SS	F Value	Pr > F
Intercept	13.28099	0.38456	1553.97961	1192.68	<.0001
Ws	-0.21855	0.08048	9.60819	7.37	0.0067
SR_	0.00101	0.00012069	90.71443	69.62	<.0001
_RH	0.06625	0.00559	182.98835	140.44	<.0001

```
Td                  0.45090    0.02050    630.39528   483.83  <.0001
```

Stepwise Selection: Step 4

Bounds on condition number: 3.1415, 36.41
----

3. Compacted sandy soil

The REG Procedure
Model: MODEL1
Dependent Variable: __mc mc

Stepwise Selection: Step 1

Variable Td Entered: R-Square = 0.6237 and C(p) = 2025.324

Analysis of Variance

Source	DF	Sum of Squares	Mean Square	F Value	Pr > F
Model	1	5031.99342	5031.99342	1897.61	<.0001
Error	1145	3036.24987	2.65175		
Corrected Total	1146	8068.24329			

Variable	Parameter Estimate	Standard Error	Type II SS	F Value	Pr > F
Intercept	14.52494	0.05081	216663	81705.8	<.0001
Td	0.43181	0.00991	5031.99342	1897.61	<.0001

Bounds on condition number: 1, 1

Stepwise Selection: Step 2

Variable _RH Entered: R-Square = 0.8611 and C(p) = 28.4747

Analysis of Variance

Source	DF	Sum of Squares	Mean Square	F Value	Pr > F
Model	2	6947.51916	3473.75958	3545.90	<.0001
Error	1144	1120.72412	0.97965		
Corrected Total	1146	8068.24329			

Variable	Parameter Estimate	Standard Error	Type II SS	F Value	Pr > F
Intercept	9.67961	0.11385	7081.96389	7229.05	<.0001
Td	0.36081	0.00624	3280.16943	3348.29	<.0001
_RH	0.12489	0.00282	1915.52574	1955.31	<.0001

Bounds on condition number: 1.071, 4.2841

Stepwise Selection: Step 3

Stepwise Selection: Step 3

Variable SR Entered: R-Square = 0.8632 and C(p) = 12.5548

```
                          Analysis of Variance

                                   Sum of          Mean
         Source             DF     Squares         Square    F Value    Pr > F

         Model               3   6964.69207     2321.56402   2404.55    <.0001
         Error            1143   1103.55122        0.96549
         Corrected Total  1146   8068.24329


                        Parameter     Standard
              Variable   Estimate       Error    Type II SS  F Value  Pr > F

              Intercept   10.50324      0.22564   2092.01540  2166.80  <.0001
              Td           0.41835      0.01498    752.67833   779.58  <.0001
              SR          -0.00054727  0.00012976   17.17290    17.79  <.0001
              _RH          0.11410      0.00380    872.53237   903.72  <.0001

                   Bounds on condition number: 6.2752, 42.672
---------------------------------------------------------------------------------

                        Stepwise Selection: Step 4


            Variable WS Entered: R-Square = 0.8644 and C(p) = 5.0000


                          Analysis of Variance

                                   Sum of          Mean
         Source             DF     Squares         Square    F Value    Pr > F

         Model               4   6973.84859     1743.46215   1819.30    <.0001
         Error            1142   1094.39469        0.95831
         Corrected Total  1146   8068.24329


                        Parameter     Standard
              Variable   Estimate       Error    Type II SS  F Value  Pr > F

              Intercept   11.10232      0.29681   1340.84158  1399.17  <.0001
              Td           0.41560      0.01495    740.17717   772.37  <.0001
              SR          -0.00050470  0.00013001   14.44129    15.07  0.0001
              _RH          0.11386      0.00378    868.56855   906.35  <.0001
              WS          -0.41280      0.13354      9.15652     9.55  0.0020

                           The REG Procedure
                            Model: MODEL1
                     Dependent Variable: __mc   mc

                        Stepwise Selection: Step 4

                   Bounds on condition number: 6.2975, 61.383
---------------------------------------------------------------------------------
```

4. Not-compacted sandy soil

```
                           The REG Procedure
                            Model: MODEL1
                     Dependent Variable: __mc   mc

                        Stepwise Selection: Step 1


            Variable Td Entered: R-Square = 0.5941 and C(p) = 1551.683


                          Analysis of Variance

                                   Sum of          Mean
         Source             DF     Squares         Square    F Value    Pr > F
```

113

```
Model                     1    4253.06988    4253.06988    1680.17    <.0001
Error                  1148    2905.96726       2.53133
Corrected Total        1149    7159.03714


                        Parameter      Standard
           Variable      Estimate        Error    Type II SS  F Value  Pr > F

           Intercept     15.21030       0.04728       261938   103479  <.0001
           Td             0.51486       0.01256    4253.06988  1680.17  <.0001

                    Bounds on condition number: 1, 1
-------------------------------------------------------------------------------

                         Stepwise Selection: Step 2


           Variable _RH Entered: R-Square = 0.8013 and C(p) = 176.7889


                            Analysis of Variance

                                   Sum of         Mean
       Source              DF      Squares       Square    F Value   Pr > F

       Model                2    5736.27186    2868.13593   2312.22   <.0001
       Error             1147    1422.76528       1.24042
       Corrected Total    1149    7159.03714


                        Parameter      Standard
           Variable      Estimate        Error    Type II SS  F Value  Pr > F

           Intercept     10.28277       0.14629    6128.31399  4940.50  <.0001
           Td             0.39693       0.00943    2197.35821  1771.46  <.0001
           _RH            0.12784       0.00370    1483.20197  1195.72  <.0001

                 Bounds on condition number: 1.1504, 4.6017
-------------------------------------------------------------------------------

                         Stepwise Selection: Step 3

                            The REG Procedure
                              Model: MODEL1
                        Dependent Variable: __mc   mc

                         Stepwise Selection: Step 3


           Variable SR Entered: R-Square = 0.8242 and C(p) = 26.1335


                            Analysis of Variance

                                   Sum of         Mean
       Source              DF      Squares       Square    F Value   Pr > F

       Model                3    5900.71353    1966.90451   1791.33   <.0001
       Error             1146    1258.32361       1.09801
       Corrected Total    1149    7159.03714


                        Parameter      Standard
           Variable      Estimate        Error    Type II SS  F Value  Pr > F

           Intercept      8.59085       0.19509    2129.23512  1939.17  <.0001
           Td             0.24866       0.01502     301.03524   274.16  <.0001
           SR             0.00108    0.00008841     164.44167   149.76  <.0001
           _RH            0.14698       0.00381    1630.81895  1485.24  <.0001

                 Bounds on condition number: 3.2955, 22.636
-------------------------------------------------------------------------------
```

114

Stepwise Selection: Step 4

Variable Ws Entered: R-Square = 0.8277 and C(p) = 5.0000

Analysis of Variance

Source	DF	Sum of Squares	Mean Square	F Value	Pr > F
Model	4	5925.63318	1481.40829	1375.23	<.0001
Error	1145	1233.40396	1.07721		
Corrected Total	1149	7159.03714			

Variable	Parameter Estimate	Standard Error	Type II SS	F Value	Pr > F
Intercept	8.02325	0.22642	1352.65433	1255.70	<.0001
Td	0.25204	0.01489	308.58136	286.46	<.0001
SR	0.00099033	0.00008961	131.55591	122.13	<.0001
_RH	0.14632	0.00378	1614.15549	1498.46	<.0001
Ws	0.34865	0.07249	24.91965	23.13	<.0001

The REG Procedure
Model: MODEL1
Dependent Variable: __mc   mc

Stepwise Selection: Step 4

Bounds on condition number: 3.3028, 35.14

APPENDIX E: DATA LABELLING SYSTEM

Data label format: Raw Collected Data

Example file name format: Sask-i-c-t.txt

First word: Site name

Second character: Replicate number (i –iii)

Third character   Compaction level (c - n)

Fourth character   Soil type (c – s)

For example a file name Sask-2-c-s contains: collected measured data in site Sask, replicate number two, compacted, sandy soil.

APPENDIX F: SOIL AND WEATHER VARIABLES DATA: CD ROM

CD ROM contains the collected raw & averaged data (replications) for all soil types and

configurations.

APPENDIX G: SENSOR CALIBRATION DATA: CD ROM

CD ROM contains the data used for thermal infrared sensor calibration.

APPENDIX H: INTERFACE™ MB-50 SPECIFICATIONS SHEET

Specifications sheet of the interface™ MB-50 mini-beam bending load cell

interface
ADVANCED FORCE MEASUREMENT

MINIBEAM LOAD CELLS

Exceptional Accuracy in Electronic Force Measurement

Model MB-5

Model MB-250

FEATURES

- Ultra Precision
- Excellent Linearity
- High Repeatability
- Low Creep
- Low Moment Sensitivity

- Thermally Compensated
- Low Cost
- Compact
- Easily Installed
- NBS Handbook 44 Sealable

RATED CAPACITIES: 5, 10, 25, 50, 75, 100, 150 and 250 pounds
(22.2N, 44N, 111N, 222N, 333N, 445N, 666N, 1112N)

Minibeam strain gage load cells offer exceptional accuracy. Eight models operate in tension or compression in controlled environments. Their compact size and cantilever beam design adapt them to a wide variety of installations.

Interface has applied its proprietary, advanced materials technology to strain gage and flexure design. The result: load cells recognized worldwide for highest accuracy in the industry yet, priced competitively with brands offering lower performance.

Minibeam electronic load cells have no moving parts. They cannot wear out or get out of adjustment. Their specifications (below) prove superior performance—a major factor in Minibeam's wide acceptance in critical applications such as: force and tensile testing; thrust measurments; OEM scale applications (to H-44, PTB and SIM requirements); conveyor scales, check weighers, counting and white scales. Their exceptional accuracy, small size and mounting ease find high acceptance in ultra precision electronic scales and laboratory instrumentation.

The Interface optional MR (Moisture Resistant) Minibeam is now available as a cost effective method of protecting 25 thru 250 lb load cells against the effects of exposure to high humidity (up to 95% RH) and periodic condensation.

SPECIFICATIONS*

Non-Linearity—%Rated Output	±0.03
Hysteresis—%Rated Output	±0.02
Non-Repeatability—%Rated Output	±0.01
Temperature Range, Compensated—°F (– 18° to 66°C)	0 to 150
Temperature Range, Operating—°F (– 54° to 93°C)	−65 to 200
Temperature Effect on Rated Output—% of Reading/100°F (% of Reading/55.6°C)	±0.08
Temperature Effect on Zero—%Rated Output/100°F (% Rated Output/55.6°C)	±0.08
Temperature Effect on Zero—%Rated Output/100°F (% Rated Output/55.6°C)	±0.12
For Moisture Resistant Models	
**Creep, After 20 Min.—% Rated Output	±0.03
Overload Ratings—% Rated Capacity	
Safe	±150
Ultimate	±500
Nominal Output—mV/V	3
Zero Balance—% Rated Output	±1
Input Resistance—Ohms	350±3.5
Output Resistance—Ohms	350±3.5
Excitation Voltage	
Recommended—VDC	10
Insulation Resistance, Bridge to Case—Megohms	5000

*Per SMA "Load Cell Terminology and Definitions"
**Creep specification is determined at rated capacity. Creep performance at reduced loads is proportional to the applied load.